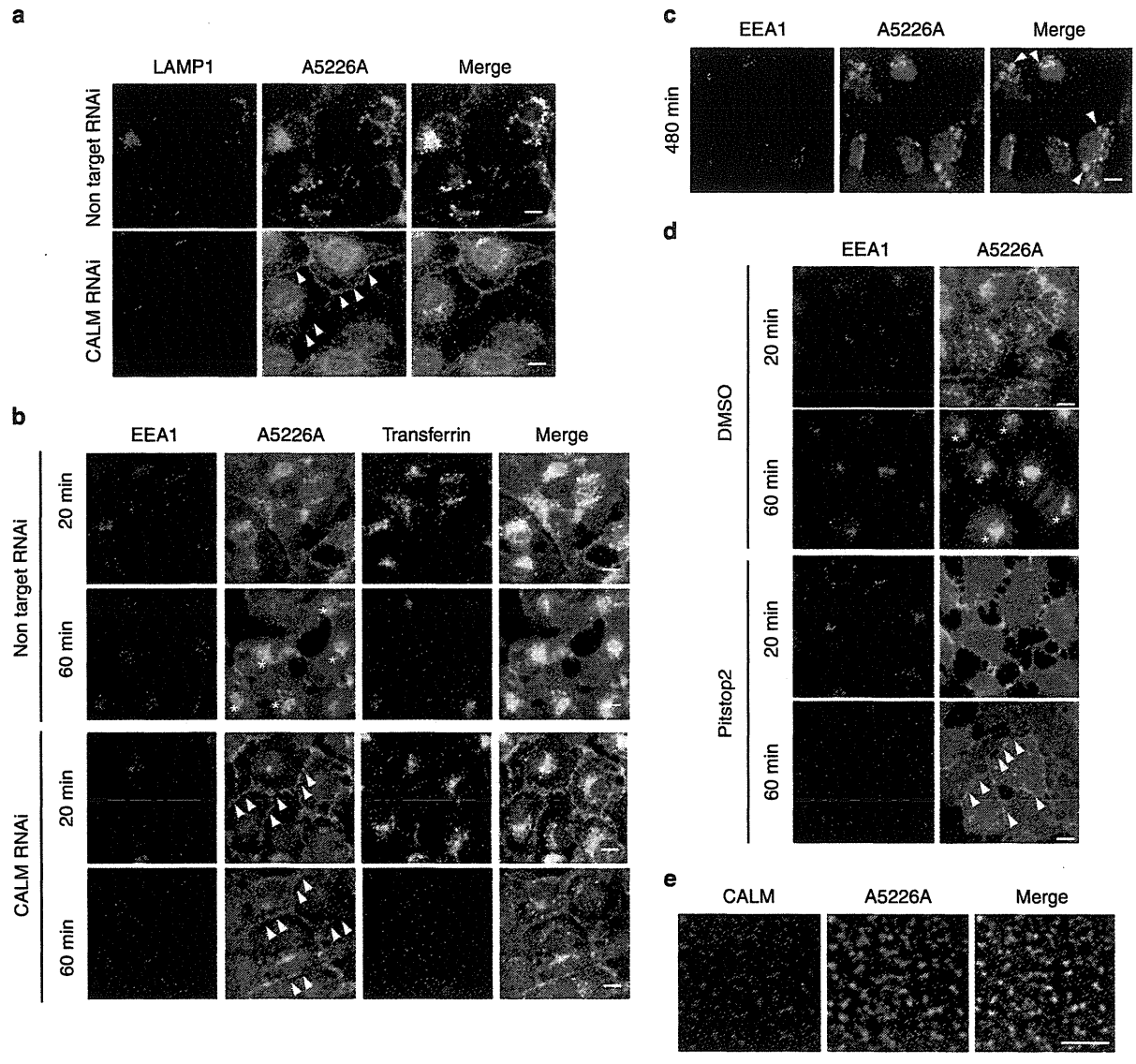

Figure 5 | CALM regulates clathrin-mediated endocytosis of γ-secretase. (**a**) HT1080 cells treated with non-target or CALM siRNA duplexes were fixed and stained with the late endosomal marker anti-LAMP1 (magenta) and anti-Nct mAb A5226A for detection of endogenous γ-secretase (green). Bar, 10 μm. (**b**) Uptake assay using Anti-Nct mAb A5226A and Alexa647-conjugated transferrin (cyan) in HT1080 cells treated with non-target or CALM siRNA duplexes. At the times indicated on the left, cells were fixed and stained with anti-EEA1 (magenta). A5226A bound to endogenous γ-secretase (green) was visualized by an Alexa488-conjugated anti-mouse IgG secondary antibody. Colocalization of the γ-secretase at EEA1-positive compartment as well as the cell surface accumulation of the γ-secretase is depicted by asterisks and arrowheads, respectively. Bar, 10 μm. (**c**) After 480 min incubation in the uptake assay, HT1080 cells were fixed and stained with anti-Nct mAb A5226A (green) and anti-EEA1 (magenta). Majority of the γ-secretase were localized at non-EEA1-positive, lysosomal compartment. Bar, 10 μm. (**d**) Uptake assay using Anti-Nct mAb A5226A (green) in DMSO or Pitstop 2 (30 μM)-treated HeLa cells. At the times indicated on the left, cells were fixed and stained with anti-EEA1 (magenta). Colocalization of the γ-secretase at EEA1-positive compartment as well as the cell surface accumulation of the γ-secretase is depicted by asterisks and arrowheads, respectively. Bar, 10 μm. (**e**) HeLa cells treated with Pitstop 2 (30 μM) for 3 h were fixed and stained with anti-Nct mAb A5226A (green) and anti-CALM (magenta). Confocal image of cell surface accumulation of the γ-secretase was taken by Leica SP5 confocal microscope. Bar, 10 μm.

Discussion

Here, we provide striking evidence for the first time that γ-secretase is constitutively internalized via clathrin-mediated endocytosis, which is regulated by CALM. The precise subcellular localization of the active γ-secretase has been enigmatic for a long time[8]. Recent studies including fly genetics revealed the prevalence of Notch processing along the endolysosomal system[10]. However, the trafficking itinerary of γ-secretase, as well as the identity of its regulatory mechanism, has rarely been described. Our results presented here clearly indicate that γ-secretase is endocytosed from the cell surface and transported to lysosomes, and that this pathway is regulated by CALM. Moreover, intriguingly, binding assay revealed that CALM directly recognizes Nct as an endocytic cargo in the γ-secretase complex. Unexpectedly, significant amount of immature Nct was detected in the ANTH domain-bound fraction, whereas mature Nct was the only species that locates at the cell surface. Considering the previous report that Nct C-terminally fused with ER-retention signal was still capable of forming active γ-secretase and maturated[39], steric hindrance of the C terminus

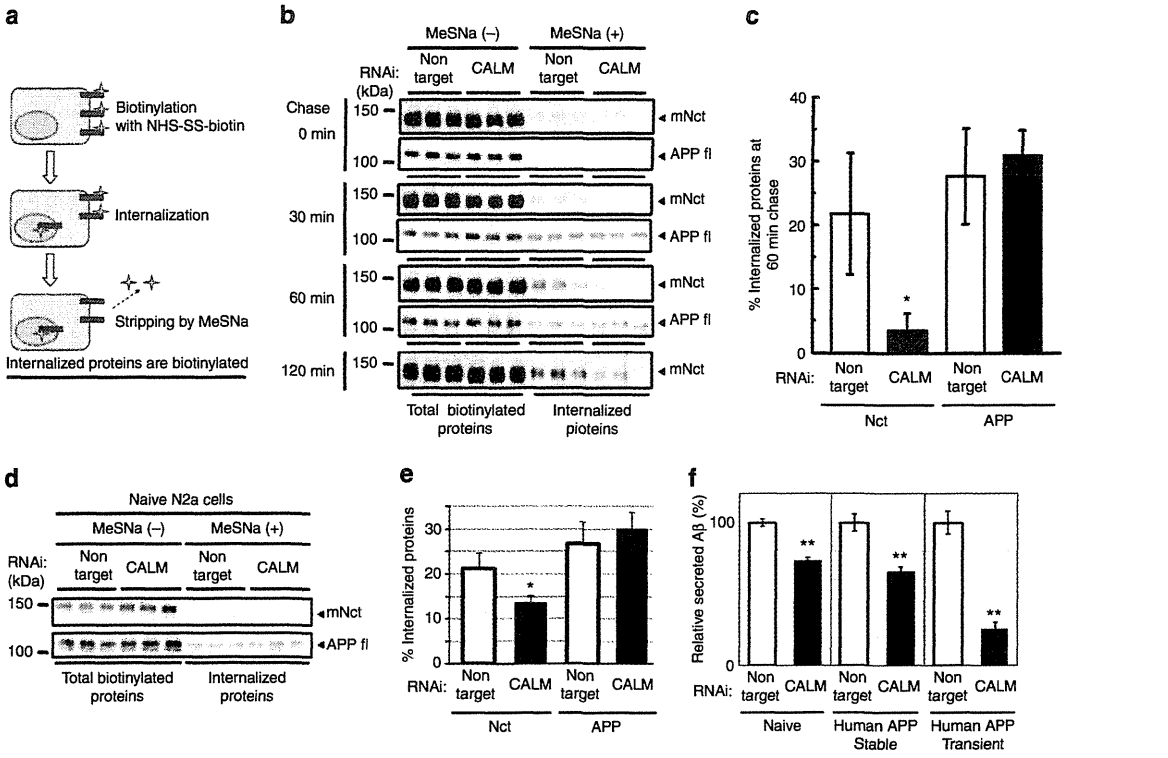

Figure 6 | Internalization of the γ-secretase is reduced by CALM knockdown. (**a**) Schematic diagram of surface biotinylation-stripping analysis to assess the rate of endocytosis using NHS-SS-Biotin. NHS-SS-biotin was cleaved by reducing reagent MeSNa to distinguish between internalized- and surface localized-proteins. (**b**) Effect of CALM RNAi on internalization of the γ-secretase and APP in HT1080 cells. Total biotinylated proteins (MeSNa (−)) as well as internalized proteins (MeSNa (+)) in the lysate were pulled down and visualized by western blotting. (**c**) Ratio of internalized proteins at 60 min chase in (**b**) ($n=3$, mean ± s.e.m., $^*P<0.05$ by Student's t-test). (**d**) Effect of CALM RNAi on internalization of the γ-secretase and APP in naive N2a cells at 30 min chase. (**e**) Ratio of internalized proteins at 60 min chase in (**d**) ($n=3$, mean ± s.e.m., $^*P<0.05$ by Student's t-test). (**f**) Effect of CALM RNAi on the levels of total secreted Aβ from naive, N2a cells stably or transiently expressing human APP measured by ELISA ($n=6$, mean ± s.e.m., $^{**}P<0.005$ compared with each non-target RNAi by Student's t-test). Human Aβ-specific ELISA system was used for the detection of Aβ from transfected human APP. Full size blots of (**b**) and (**d**) can be found in Supplementary Fig. 1.

of Nct would have occurred upon the assembly of the complex. This raises the possibility that as yet unknown signal or post-translational modifications induce a structural change in the cytoplasmic domain of Nct and allow the binding to CALM, resulting in enhanced endocytosis. We have also shown that the extents of reduction in total Aβ secretion from endogenous, stably expressed and transiently expressed APP were varied (Fig. 6f). Total Aβ production is correlated with β-cleavage that requires endocytosis of APP[40]. Thus, overexpressed APP might overflow into the clathrin-coated pits regulated by CALM. This might be a reason why significant reduction in Aβ secretion was observed in knockdown experiments by Xiao *et al.*[19] as well as the transient expression of APP (Fig. 6f). However, Aβ42 ratio was altered in heterozygous knockout mice brains, while total Aβ level was unchanged, suggesting that the alteration of the γ-secretase activity is more sensitive than that of APP. As to the physiological significance of this CALM-dependent γ-secretase endocytosis, it has been shown that Notch S3 processing by γ-secretase at the cell surface produces stable NICD starting at Val residue, whereas its endosomal processing produces shorter, unstable NICD leading to the attenuated signalling[41]. This implies that the magnitude of Notch signalling is controlled not only by the trafficking of Notch itself but also that of γ-secretase. Whether γ-secretase activity is regulated by membrane traffic in response to specific signalling pathways will be an important area for further investigation.

Also intriguing is the finding that loss of CALM alters proteolytic activity of γ-secretase to reduce the production ratio of Aβ42, consistently observed both *in vitro* and *in vivo*. To date, several protective mutations/variants against AD have been reported by genome-wide association studies and whole-genome sequencing. Among these variants, a rare variant causing A673T substitution of *APP* gene reduced Aβ production by affecting β-cleavage[42], and minor allele (A) of rs3865444 in *CD33* gene regulated the phagocytosis of Aβ by microglia[43,44]. Considering the fact that almost all of FAD-linked mutations increase the production/aggregation of Aβ *in vitro* as well as *in vivo*, modulation of brain Aβ levels is crucial to the molecular aetiology of AD. However, no genetic variant altering the γ-secretase activity has been reported, although γ-secretase modulator has been regarded as a promising treatment[1]. Our present result suggests that the minor allele (A) of rs10792832 near *PICALM* gene would affect the expression of CALM in a way to reduce the production ratio of Aβ42, thereby leading to a protective effect against AD[12]. Importantly, reduced Aβ42/total Aβ ratio was recapitulated by treatment with YM201636 that blocks endosomal maturation and redistributes γ-secretase to the earlier endocytic compartment. These results suggest that the change in the steady-state localization of γ-secretase, which is determined by the balance between endolysosomal trafficking and recycling to the cell surface, is correlated with the lowered Aβ42/total Aβ ratio. Notably, in YM201636 treated cells, we did

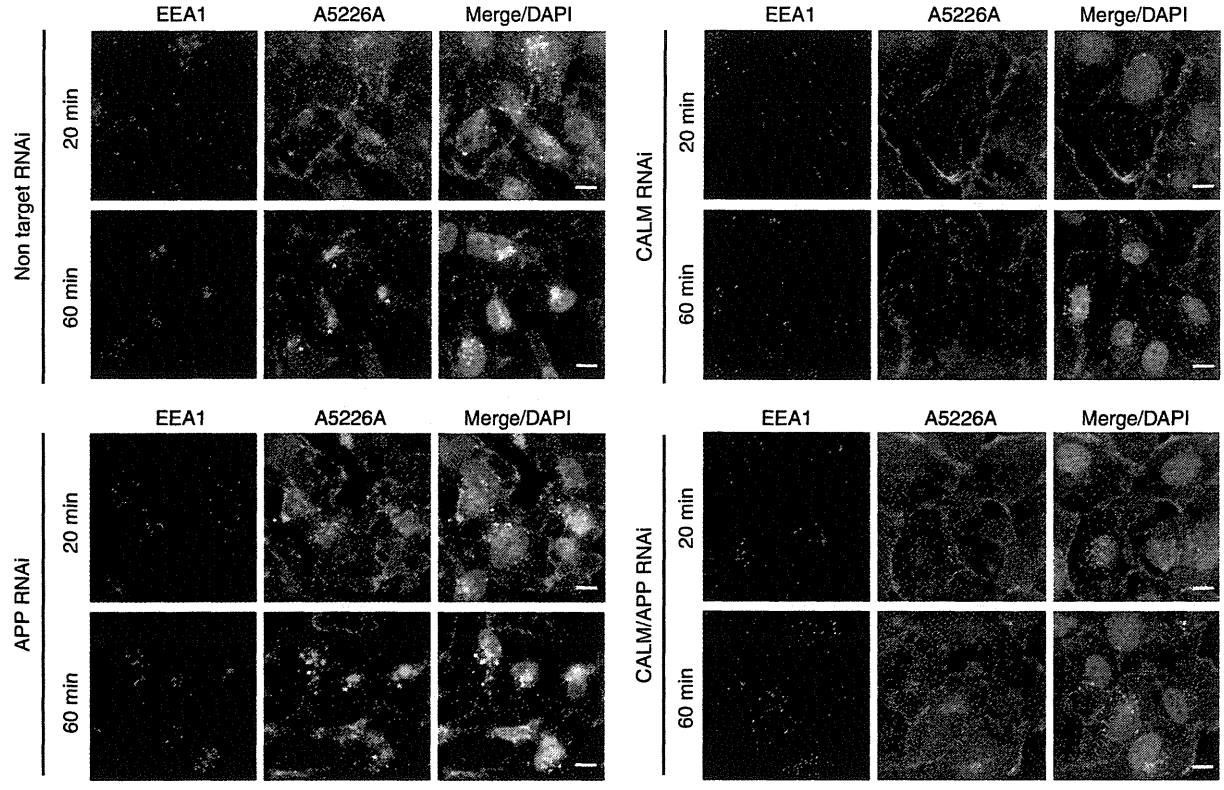

Figure 7 | APP knockdown unaffected the endocytosis of the γ-secretase. Uptake assay using Anti-Nct mAb A5226A in HT1080 cells treated with non-target, CALM or APP siRNA. At the times indicated on the left cells were fixed and stained with anti-EEA1 (magenta) as Fig. 5. Colocalization of the γ-secretase at EEA1-positive compartment are depicted by asterisks. Bar, 10 μm.

not observe changes in the total level of Aβ secretion, while incubation of membrane fractions obtained from YM201636-treated cells increased the production of Aβ. It is tempting to speculate that the endolysosomal maturation is required for not only the production but also secretion of Aβ. Nevertheless, CALM depletion appears to shift the balance towards recycling, so that γ-secretase accumulates at the earlier endocytic compartment where it preferentially cleaves APP CTF at Aβ40 position. Why does this change in localization matter? It has been shown biochemically that subcellular localization affects the proteolytic activity of γ-secretase and this might be attributed to the difference in membrane lipid composition or pH[41,45,46]. As shown in this study, low pH caused a significant increase in Aβ42/total Aβ ratio in an *in vitro* assay, indicating that alteration of pH along with endosomal maturation has an impact on the γ-secretase activity for Aβ42 production ratio. Our findings also raise the possibility that inhibition of CALM function as well as of endosomal maturation of γ-secretase is considered as a promising therapeutic target of AD.

While total systemic loss of CALM in mice leads to neonatal death possibly due to impaired iron uptake and other crucial endocytosis, heterozygous mice showed no obvious abnormalities[20]. Reduced Aβ42/total Aβ ratio in heterozygous mouse brain suggests that partial inhibition of CALM function could be enough to prevent the development of AD with minimal side effects. In this regard, it is noteworthy to mention that Ca^{2+}-dependent synaptic vesicle exocytosis has been shown to modulate PS1 conformation and the Aβ42 production ratio[47]. As CALM is essential to the endocytic pathway of synaptic vesicles[48], CALM would be a critical regulator of neuronal activity-dependent Aβ42 production ratio. Notably, the magnitude of reduction in Aβ42 ratio by CALM knockdown varied with different APP constructs (Compare Figs 2b,e and 3c). One possibility is that subcellular location of β-cleavage of APP, which should precede the γ-cleavage, is correlated with this difference in the reduction of Aβ42 ratio. In fact, recent studies indicate that β-cleavage of APP is dynamically regulated by membrane trafficking[49–51] as well as neuronal activity[40,52].

SNPs found in the late-onset AD patients are associated with the disease with a reduced risk, so it would be interesting to see whether the expression level or function of CALM is lowered in the brains of patients carrying these SNPs. CALM knockdown slowed, but did not abolish, the endocytosis of the γ-secretase, suggesting that other factors or molecular systems including AP180 would complement the trafficking of the γ-secretase upon depletion of CALM function within cells. In summary, we have identified CALM as a regulator of γ-secretase endocytosis and Aβ42 production ratio. This study is an important step forward in understanding the cell biology of γ-secretase as well as defining a novel target for the anti-amyloid treatment of AD.

Methods

Molecular biology. Human CALM (long (CALM-L) and short (CALM-S) isoforms, NCBI nucleotide accession number BC048259 and BC064357, respectively) and human BACE1 (BC065492) ORFs were amplified from IMAGE clones (Open Biosystems) using KOD plus neo DNA polymerase (TOYOBO). Expression constructs encoding wild-type human APP_{695} full length and C99 were described before[27]. Mammarian expression constructs were made using pEF6-V5 His TOPO TA or pcDNA3.1-hygro vector (Invitrogen). Bacterial expression constructs for recombinant GST fusion proteins were made using pFAT2 vector encoding Hisx6-Gultathion S transferase (GST). The following ON-TARGETplus SMARTpool small interfering RNAs (Thermo Scientific) were used against human Nct (#L-008043-00), human APP (#L-003731-00), mouse APP (#L-043246-00), human CALM (#L-004004-00), mouse CALM (#L-041440-01). Luciferase GL2

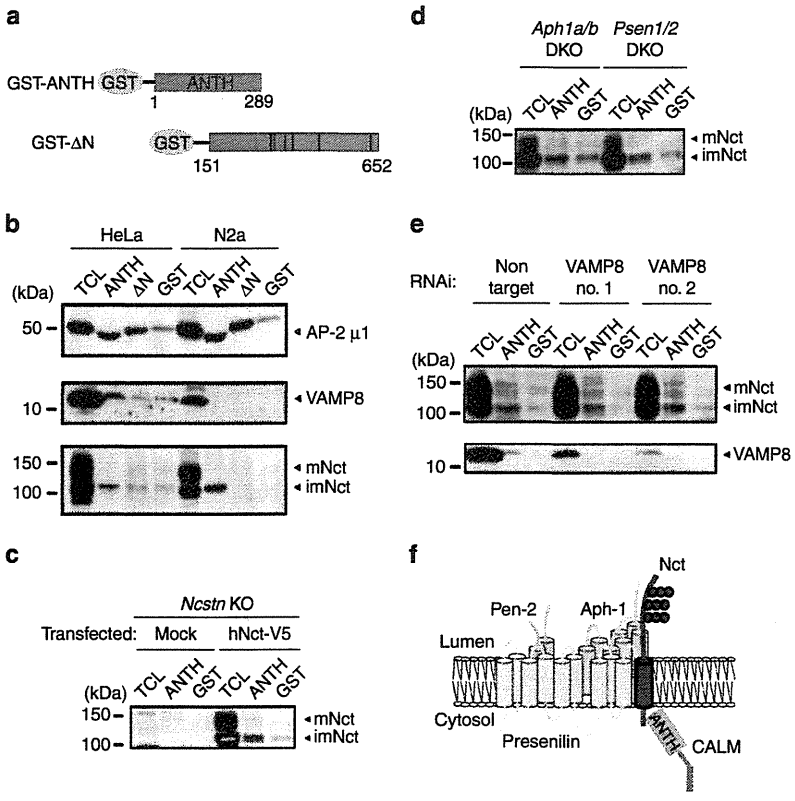

Figure 8 | CALM directly recognizes γ-secretase. (**a**) Schematic depiction of recombinant proteins used in this study. (**b**) GST pull-down assay using HeLa or N2a cell lysates. Bound proteins were analysed by western blotting using antibodies against AP-2, VAMP8 and Nct (mNct, mature Nct; imNct, immature Nct). (**c**) GST pull-down assay using lysates from *Ncstn* knockout fibroblast cells expressing mock or human Nct with C-terminal V5 tag. (**d**) GST pull-down assay using lysates from *Aph1a/b* DKO and *Psen1/2* DKO fibroblast cells. (**e**) Effect of VAMP8 knockdown on the interaction between CALM and Nct. Two different siRNAs were treated with HeLa cells, and GST pull-down assay was performed as in (**a**). (**f**) Schematic depiction of the binding of CALM and Nct in the γ-secretase complex. Full size blots of (**b**–**e**) can be found in Supplementary Fig. 1.

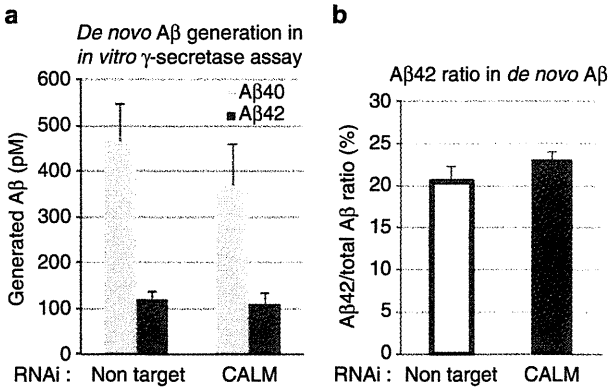

Figure 9 | Intrinsic enzymatic activity of the γ-secretase in CALM-depleted cell membranes. Levels of *de novo* Aβ generation (**a**) and Aβ42/total Aβ ratio (**b**) in *in vitro* γ-secretase assay using cell membrane treated with non-target or CALM siRNA duplexes ($n=3$, mean ± s.e.m).

(#D-001100-20) and Non-targeting pool (#D-001810-10) were used as control siRNAs. SiRNAs targeting human VAMP8 (SI 02652993 and SI04437804) were purchased from Qiagen.

Antibodies and chemicals. The following antibodies were purchased from commercial suppliers: anti-CALM (sc-6433, Santa Cruz, 1:1,000 dilution for western blot analyses, 1:400 dilution for immunocytochemical analysis), anti-APPc (#18961, Immuno-Biological Laboratories, 1:1,000), anti-human Aβ specific antibody 82E1 (#10323, Immuno-Biological Laboratories, 1:1,000 dilution), anti-α-tubulin DM1A (T6199, Sigma, 1:2,000 dilution), anti-Nct N terminus (sc-14369, N-19; Santa Cruz, 1:1,000 dilution), anti-Nct C terminus (N1660, Sigma, 1:1,000 dilution), anti-LAMP1 (#328611, Alexa-647 tagged antibody, Bio Legend, 1:500 dilution), anti-EEA1 (#2411S, Cell Signaling Technology, 1:200 dilution), anti-AP-2μ1 (#2386-1, Epitomics, 1:1,000 dilution), anti-VAMP8 (ab76021, Abcam, 1:5,000 dilution). Rabbit polyclonal anti-PS1 CTF antibody G1L3 and mouse monoclonal anti-Nct A5226A were described previously[31,53]. Pitstop 2 and YM201636 were purchased from Abcam and Cayman Chemicals, respectively.

Cell culture and RNA interference. HeLa S3 (#CCL-2.2, ATCC), Neuro2a (N2a) (#CCL-131, ATCC), HT1080 (provided from Dr. Masatoshi Maki (Nagoya University)), HEK293 (#CCL-1573, ATCC), embryonic fibroblast cells obtained from *Ncstn*$^{-/-}$, *Psen1*$^{-/-}$;*Psen2*$^{-/-}$ *and Aph1a*$^{-/-}$;*Aph1b*$^{-/-}$ mice (*Ncstn* KO, *Psen1/2* DKO and *Aph1a/b* DKO MEFs, respectively)[54–56] were cultured in DMEM supplemented with 10% fetal calf serum. N2a cells stably expressing human wild-type APP_{695} were selected using 50 μg ml^{-1} Blasticidin S (Calbiochem). Flp-In T-REx-293 cell lines stably expressing Tet-inducible human wild-type APP_{695} were selected using 200 μg ml^{-1} Hygromycin according to the manufacturer's protocol (Invitrogen). *Ncstn* KO MEF cells stably expressing V5/His-tagged Nct were selected using 10 μg ml^{-1} Blasticidin (Calbiochem)[57]. siRNAs were transfected into 20∼30% confluent cells using LipofectAMINE RNAiMAX (Invitrogen) at a concentration of 20 nM, and cells and culture medium were analysed 48–72 h after transfection. In experiments in which a combination of siRNA and plasmid delivery was necessary, plasmids were transfected with TransIT-2020 (Mirus) or Fugene 6 (Roche Applied Science) 24 h after siRNA delivery.

For immunocytochemical analysis, cells cultured on glass coverslips were fixed for 15 min in 4% paraformaldehyde and then permeabilized with 0.2% Tx-100 for 10 min. All solutions were made in PBS. Coverslips were then incubated with primary antibodies as indicated for 1 h. After washing with PBS, coverslips were incubated with secondary antibodies for 1 h and washed with PBS, mounted on slide glass using PermaFluor Aqueous Mounting Medium (Thermo Scientific) mixed with 1 μg ml^{-1} DAPI for nuclear staining. Images were collected with either

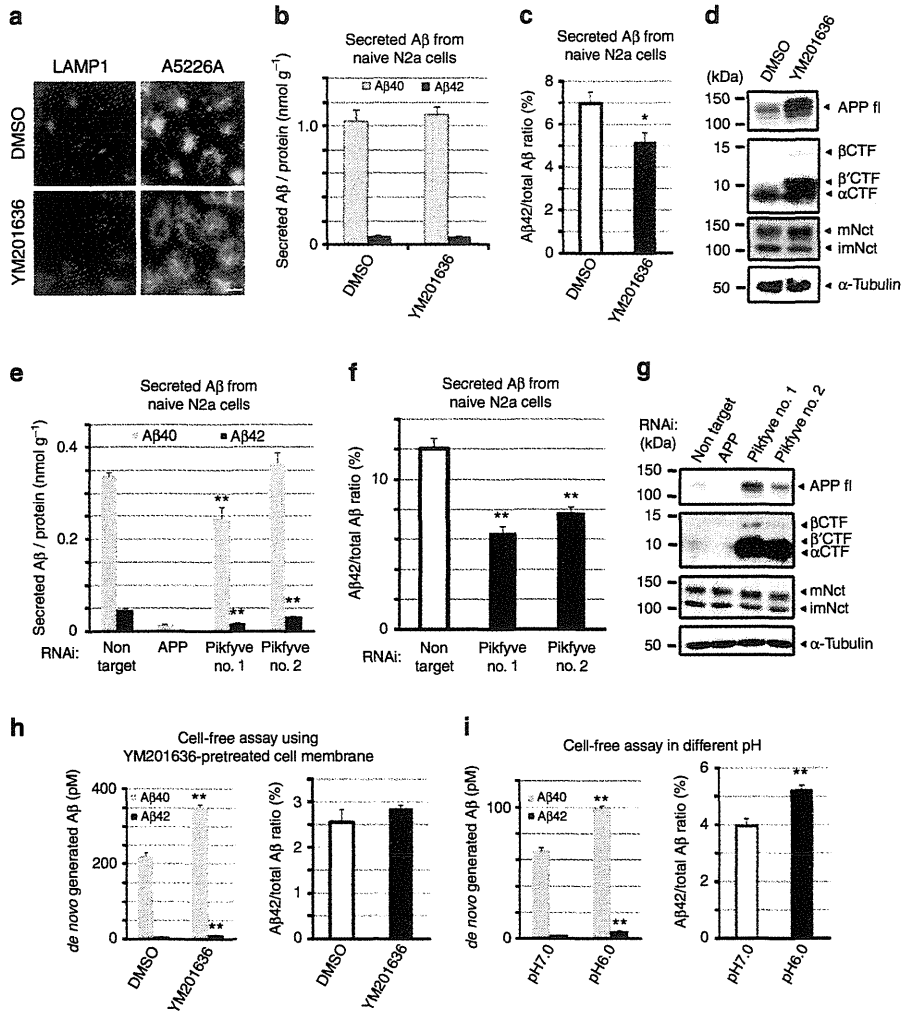

Figure 10 | Acidification in the consequence of endosomal maturation is the critical determinant for Aβ42 ratio. (**a**) Effect of YM201636 on the localization of LAMP1-positive compartment and the endogenous γ-secretase in HeLa cells. Bar, 10 μm. (**b**,**c**) Levels of secreted Aβ from N2a cells ($n=3$, mean ± s.e.m) (**b**) and Aβ42/total Aβ ratio (**c**) treated with DMSO or YM201636 ($n=3$, mean ± s.e.m., $^*P<0.05$ by Student's *t*-test). (**d**) N2a cells treated with DMSO or YM201636 were analysed by western blotting with antibodies to APP, Nct and α-tubulin (mNct, mature Nct; imNct, immature Nct). (**e**,**f**) Effect of knockdown of Pikfyve on secreted Aβ levels from N2a cells ($n=6$, mean ± s.e.m., $^{**}P<0.005$ by Student's *t*-test) (**e**), Aβ42/total Aβ ratio (**f**) ($n=6$, mean ± s.e.m., $^{**}P<0.005$ by Student's *t*-test). (**g**) N2a cells treated with APP or Pikfyve siRNA duplexes were analysed by western blotting with antibodies to APP, Nct and α-tubulin. (**h**) Levels (*left*) and Aβ42/total Aβ ratio (*right*) in *de novo* Aβ generated in cell-free assay using membranes obtained from APP_{695}-expressing HEK293 cells pretreated with DMSO or YM201636 ($n=3$, mean ± s.e.m., $^{**}P<0.005$ by Student's *t*-test). (**i**) Levels (*left*) and Aβ42/total Aβ ratio (*right*) in *de novo* Aβ generated in cell-free assay using APP_{695}-expressing HEK293 cell membranes under different pH condition (7.0 or 6.0) ($n=3$, mean ± s.e.m., $^{**}P<0.005$ by Student's *t*-test). Full size blots for (**d**) and (**g**) can be found in Supplementary Fig. 1.

a fluorescence microscope (AxioObserver Z1, Zeiss) with a × 40 Plan Apochromat oil immersion objective of NA 1.3, AxioVision software or a confocal microscope (SP5, Leica) with a × 63 PL APO CS oil immersion objective of NA 1.4, Leica LAS AF software. Images were cropped and processed using ImageJ software (NIH). To detect colocalization of CALM and Nct, subconfluent cells were treated with 30 μM Pitstop 2 in DMEM without FBS for 3 h before fixation.

For western blot analyses, cells were lysed by Laemlli sample buffer and sonicated. Protein concentration was measured by using BCA protein assay (Pierce). For detection of APP CTFs, cell lysates (40 mg of protein) were dephosphorylated by recombinant Lambda protein phosphatase (400 unit; New England Biolabs) for 4 h at 30 °C (ref. 58). Secreted human Aβ was separated in Urea-SDS PAGE gel[59] and detected by western blotting using a human Aβ specific antibody 82E1.

Brain extraction. All experiments using animals in this study were performed according to the guidelines provided by the Institutional Animal Care Committee of Graduate School of Pharmaceutical Sciences, The University of Tokyo. All animals (5-month-old mice, female) were maintained on food and water with a 12 h light/dark cycle. The brains that were excised from 5 months old of *Picalm*$^{+/-}$ or wild-type mice were homogenized in RIPA buffer (Thermo Scientific) containing Complete protease inhibitor cocktail (Roche Applied Science). Homogenates were cleared by centrifugation at 200,000 × *g* for 20 min at 4 °C, and the resultant supernatant was collected as brain RIPA extract. The RIPA extract was used for quantitation of Aβ by ELISA (Human/Rat beta-Amyloid (40) ELISA Kit (#294-62501, WAKO Pure Chemical Industries) and Human/Rat β-Amyloid (42) ELISA Kit, High Sensitivity (#292-64501, WAKO Pure Chemical Industries) and also analysed by SDS-PAGE and western blots. For *in vitro* BACE1 assay, the RIPA extract was acidified by 25 mM CH_3COONa pH 4.5 and incubated with the β-secretase-specific recombinant peptide-based substrate JMV2236 (Bachem) at 37 °C at the indicated times. Fluorescence of the fractions was measured at 320 and 420/430 nm as excitation and emission wavelengths, respectively[60].

Ligand uptake assays. Subconfluent HeLa or HT1080 cells were incubated in the medium containing 50 μg ml^{-1} Alexa-647 transferrin and 10 μg ml^{-1} anti-Nct MAb A5226A for 20 min at 37 °C. After washing with medium, fresh prewarmed medium was added and further incubated for varying times at 37 °C. Cells were then washed immediately with PBS, fixed in PFA and processed for immunocytochemical analysis.

Cell-surface biotinylation-based endocytosis assay. Cell-surface biotinylation-based endocytosis assay was performed according to the method established by Bretscher and Lutter[61] with some modifications. In brief, near-confluent cells were washed with ice-cold PBS and then incubated on ice with a membrane-impermeant, cleavable biotin derivative Sulfo-NHS-SS-Biotin (Thermo Scientific, 1 mg ml^{-1} in PBS) for 30 min to label surface proteins. Excess biotin reagent was quenched by washing cells three times with 0.1 M glycine in PBS. Cells were rinsed with ice-cold PBS and re-fed with prewarmed and CO_2 equilibrated growth medium including 20 μM GM6001 (Calbiochem) (except for 't0' sample). Cells were then incubated for varying times at 37 °C to allow internalization. At each time point, cells were transferred to ice to terminate internalization, washed with ice-cold PBS twice and then stripped of remaining surface biotin by washing three times for 20 min on ice in biotin-stripping buffer (50 mM Tris pH 8.6, 100 mM NaCl, 1 mM EDTA and 0.2% purified BSA, 100 mM sodium 2-mercapto-ethanesulfonate (MeSNa)). After quenching MeSNa by incubating for 10 min on ice in PBS containing 120 mM Iodoacetic acid followed by washing with ice-cold PBS twice, cells were lysed in PBS containing 1% SDS. The lysates were then sonicated and biotinylated proteins were captured with streptavidin sepharose (GE Healthcare) for 12 h on a rotary mixer, eluted in SDS sample buffer by boiling for 1 min and analysed by western blotting.

Protein expression and purification. CALM ANTH domain (1–289) and ΔN protein (151–652) were expressed as His- GST-fusion proteins in *Escherichia coli* BL21(DE3) (WAKO). Cells were grown to mid log, induced with 0.2 mM IPTG for 2.5 h at 37 °C. Bacterial lysates were prepared from pellets by sonication in *E coli* lysis buffer (20 mM Tris–HCl pH8.0, 300 mM NaCl, 20 mM imidazole, 0.1% Triton X-100), cleared by centrifugation and His-GST-fusion proteins were purified on Ni-NTA agarose (Qiagen) in 20 mM Tris–HCl pH 8.0, 300 mM NaCl, 20 mM Imidazole and eluted in the same buffer but now containing 200 mM imidazole. Proteins were dialysed against Tris-buffered saline (50 mM Tris–HCl pH8.0, 150 mM NaCl) and then aliquots were frozen in liquid nitrogen for storage at − 80 °C. HeLa, N2a and *Ncstn* KO MEF cell lysates were prepared by using mammalian cell lysis buffer (20 mM Tris–HCl, pH 7.6, 150 mM NaCl, 0.5% Triton X-100) containing Complete protease inhibitor cocktail and precleared by incubating with glutathione sepharose (GE Healthcare) for 1 h. In pull-down experiments, 1 mg of cleared total cell lysate and 200 μg of GST-CALM proteins were mixed in lysis buffer. Following the addition of 50 μl glutathione sepharose beads, the mixture was incubated for 90 min at 4 °C on a rotator. The glutathione sepharose beads were washed three times with lysis buffer. After washing, 100 μl of 2 × sample buffer was added to the beads for elution and boiled for 1 min. Bound proteins were analysed by SDS-PAGE and western blots. GST alone served as a negative control.

***In vitro* γ-secretase assays.** For secreted Aβ levels, conditioned media from N2a cells, HEK293 cells stably expressing wild-type human APP_{695} or HeLa cells co-expressing wild-type human APP_{695} and BACE1 were analysed by two-site enzyme-linked immunosorbent assay (ELISA)[62]. For cell-free γ-secretase assay, membranes of HEK293 cells stably expressing APP were collected and analysed as described previously[63]. In all, 2.5 mg ml^{-1} microsomes in homogenize buffer (20 mM HEPES pH 7.0, 140 mM KCl, 250 mM sucrose, 5 mM EGTA) containing 0.5 mM DIFP, 0.5 mM PMSF, 1 μg ml^{-1} TLCK, 1 μg ml^{-1} antipain, 1 μg ml^{-1} leupeptin, 10 μg ml^{-1} phosphoramidon, 1 mM EGTA, 5 mM EDTA, 5 mM 1,10-Phenanthroline were preincubated with L-685,458 or DMSO on ice for 30 min. Microsomes were incubated at 37 °C for 6 h and then centrifuged at 15,000 rpm for 10 min. The supernatant was analysed by ELISA. In experiments in which cell-free γ-secretase assays were performed under different pH conditions, citric acid-Na_2HPO_4 buffer was used instead of HEPES buffer. For *in vitro* γ-secretase assay, 1% CHAPSO-solubilized membranes from HeLa cells were incubated with APP-based recombinant substrate C100-Flag/Myc/His purified from *Escherichia coli* under 0.25% CHAPSO condition[6,64] and then analysed by ELISA.

Statistical analysis. Data are presented as mean values and error bars indicate s.e.m. The treatment groups were compared by two-tailed Student's *t*-test. Significance was set at $^*P<0.05$ and $^{**}P<0.005$.

References

1. Holtzman, D. M., Morris, J. C. & Goate, A. M. Alzheimer's disease: the challenge of the second century. *Sci. Transl. Med.* **3,** 77sr71 (2011).
2. Tomita, T. Secretase inhibitors and modulators for Alzheimer's disease treatment. *Expert Rev. Neurother.* **9,** 661–679 (2009).
3. Tomita, T. & Iwatsubo, T. Structural biology of presenilins and signal peptide peptidases. *J. Biol. Chem.* **288,** 14673–14680 (2013).
4. Iwatsubo, T. *et al.* Visualization of A beta 42(43) and A beta 40 in senile plaques with end-specific A beta monoclonals: evidence that an initially deposited species is A beta 42(43). *Neuron* **13,** 45–53 (1994).
5. Li, Y. M. *et al.* Photoactivated gamma-secretase inhibitors directed to the active site covalently label presenilin 1. *Nature* **405,** 689–694 (2000).
6. Takasugi, N. *et al.* The role of presenilin cofactors in the gamma-secretase complex. *Nature* **422,** 438–441 (2003).
7. De Strooper, B. & Annaert, W. Novel research horizons for presenilins and gamma-secretases in cell biology and disease. *Ann. Rev. Cell Dev. Biol.* **26,** 235–260 (2010).
8. Morohashi, Y. & Tomita, T. Protein trafficking and maturation regulate intramembrane proteolysis. *Biochim. Biophys. Acta* **1828,** 2855–2861 2013.
9. Pasternak, S. H. *et al.* Presenilin-1, nicastrin, amyloid precursor protein, and gamma-secretase activity are co-localized in the lysosomal membrane. *J. Biol. Chem.* **278,** 26687–26694 (2003).
10. Vaccari, T., Lu, H., Kanwar, R., Fortini, M. E. & Bilder, D. Endosomal entry regulates Notch receptor activation in Drosophila melanogaster. *J. Cell Biol.* **180,** 755–762 (2008).
11. Harold, D. *et al.* Genome-wide association study identifies variants at CLU and PICALM associated with Alzheimer's disease. *Nat. Genet.* **41,** 1088–1093 (2009).
12. Lambert, J. C. *et al.* Meta-analysis of 74,046 individuals identifies 11 new susceptibility loci for Alzheimer's disease. *Nat. Genet.* **45,** 1452–1458 (2013).
13. Dreyling, M. H. *et al.* The t(10;11)(p13;q14) in the U937 cell line results in the fusion of the AF10 gene and CALM, encoding a new member of the AP-3 clathrin assembly protein family. *Proc. Natl Acad. Sci.USA* **93,** 4804–4809 (1996).
14. Tebar, F., Bohlander, S. K. & Sorkin, A. Clathrin assembly lymphoid myeloid leukemia (CALM) protein: localization in endocytic-coated pits, interactions with clathrin, and the impact of overexpression on clathrin-mediated traffic. *Mol. Biol. Cell* **10,** 2687–2702 (1999).
15. Meyerholz, A. *et al.* Effect of clathrin assembly lymphoid myeloid leukemia protein depletion on clathrin coat formation. *Traffic* **6,** 1225–1234 (2005).
16. Miller, S. E. *et al.* The molecular basis for the endocytosis of small R-SNAREs by the clathrin adaptor CALM. *Cell* **147,** 1118–1131 (2011).
17. Jun, G. *et al.* Meta-analysis confirms CR1, CLU, and PICALM as alzheimer disease risk loci and reveals interactions with APOE genotypes. *Arch. Neurol.* **67,** 1473–1484 (2010).
18. Treusch, S. *et al.* Functional links between Abeta toxicity, endocytic trafficking, and Alzheimer's disease risk factors in yeast. *Science* **334,** 1241–1245 (2011).
19. Xiao, Q. *et al.* Role of phosphatidylinositol clathrin assembly lymphoid-myeloid leukemia (PICALM) in intracellular amyloid precursor protein (APP) processing and amyloid plaque pathogenesis. *J. Biol. Chem.* **287,** 21279–21289 (2012).
20. Suzuki, M. *et al.* The clathrin assembly protein PICALM is required for erythroid maturation and transferrin internalization in mice. *PLoS One* **7,** e31854 (2012).
21. Duff, K. *et al.* Increased amyloid-beta42(43) in brains of mice expressing mutant presenilin 1. *Nature* **383,** 710–713 (1996).
22. Nakano, Y. *et al.* Accumulation of murine amyloidbeta42 in a gene-dosage-dependent manner in PS1 'knock-in' mice. *Eur. J. Neurosci.* **11,** 2577–2581 (1999).
23. Saito, T. *et al.* Potent amyloidogenicity and pathogenicity of Abeta43. *Nat. Neurosci.* **14,** 1023–1032 (2011).
24. Yu, H. *et al.* APP processing and synaptic plasticity in presenilin-1 conditional knockout mice. *Neuron* **31,** 713–726 (2001).
25. Cai, H. *et al.* BACE1 is the major beta-secretase for generation of Abeta peptides by neurons. *Nat. Neurosci.* **4,** 233–234 (2001).
26. Roberds, S. L. *et al.* BACE knockout mice are healthy despite lacking the primary beta-secretase activity in brain: implications for Alzheimer's disease therapeutics. *Hum. Mol. Genet.* **10,** 1317–1324 (2001).
27. Iwata, H., Tomita, T., Maruyama, K. & Iwatsubo, T. Subcellular compartment and molecular subdomain of beta-amyloid precursor protein relevant to the Abeta 42-promoting effects of Alzheimer mutant presenilin 2. *J. Biol. Chem.* **276,** 21678–21685 (2001).
28. Chyung, J. H., Raper, D. M. & Selkoe, D. J. Gamma-secretase exists on the plasma membrane as an intact complex that accepts substrates and effects intramembrane cleavage. *J. Biol. Chem.* **280,** 4383–4392 (2005).
29. Kaether, C., Schmitt, S., Willem, M. & Haass, C. Amyloid precursor protein and Notch intracellular domains are generated after transport of their precursors to the cell surface. *Traffic* **7,** 408–415 (2006).
30. Burgos, P. V. *et al.* Sorting of the Alzheimer's disease amyloid precursor protein mediated by the AP-4 complex. *Dev. Cell* **18,** 425–436 (2010).
31. Hayashi, I. *et al.* Neutralization of the gamma-secretase activity by monoclonal antibody against extracellular domain of nicastrin. *Oncogene* **31,** 787–798 (2012).
32. von Kleist, L. *et al.* Role of the clathrin terminal domain in regulating coated pit dynamics revealed by small molecule inhibition. *Cell* **146,** 471–484 (2011).
33. Carter, L. L., Redelmeier, T. E., Woollenweber, L. A. & Schmid, S. L. Multiple GTP-binding proteins participate in clathrin-coated vesicle-mediated endocytosis. *J. Cell Biol.* **120,** 37–45 (1993).

34. Tian, Y., Chang, J. C., Fan, E. Y., Flajolet, M. & Greengard, P. Adaptor complex AP2/PICALM, through interaction with LC3, targets Alzheimer's APP-CTF for terminal degradation via autophagy. *Proc. Natl Acad. Sci. USA* **110,** 17071–17076 (2013).
35. Huang, F., Khvorova, A., Marshall, W. & Sorkin, A. Analysis of clathrin-mediated endocytosis of epidermal growth factor receptor by RNA interference. *J. Biol. Chem.* **279,** 16657–16661 (2004).
36. Harel, A., Mattson, M. P. & Yao, P. J. CALM, a clathrin assembly protein, influences cell surface GluR2 abundance. *Neuromol. Med.* **13,** 88–90 (2011).
37. Harel, A., Wu, F., Mattson, M. P., Morris, C. M. & Yao, P. J. Evidence for CALM in directing VAMP2 trafficking. *Traffic* **9,** 417–429 (2008).
38. Jefferies, H. B. *et al.* A selective PIKfyve inhibitor blocks PtdIns(3,5)P(2) production and disrupts endomembrane transport and retroviral budding. *EMBO Rep.* **9,** 164–170 (2008).
39. Capell, A. *et al.* Gamma-secretase complex assembly within the early secretory pathway. *J. Biol. Chem.* **280,** 6471–6478 (2005).
40. Das, U. *et al.* Activity-induced convergence of APP and BACE-1 in acidic microdomains via an endocytosis-dependent pathway. *Neuron* **79,** 447–460 (2013).
41. Tagami, S. *et al.* Regulation of Notch signaling by dynamic changes in the precision of S3 cleavage of Notch-1. *Mol. Cell. Biol.* **28,** 165–176 (2008).
42. Jonsson, T. *et al.* A mutation in APP protects against Alzheimer's disease and age-related cognitive decline. *Nature* **488,** 96–99 (2012).
43. Bradshaw, E. M. *et al.* CD33 Alzheimer's disease locus: altered monocyte function and amyloid biology. *Nat. Neurosci.* **16,** 848–850 (2013).
44. Griciuc, A. *et al.* Alzheimer's disease risk gene CD33 inhibits microglial uptake of amyloid beta. *Neuron* **78,** 631–643 (2013).
45. Fukumori, A. *et al.* Presenilin-dependent gamma-secretase on plasma membrane and endosomes is functionally distinct. *Biochemistry* **45,** 4907–4914 (2006).
46. Holmes, O., Paturi, S., Ye, W., Wolfe, M. S. & Selkoe, D. J. Effects of membrane lipids on the activity and processivity of purified gamma-secretase. *Biochemistry* **51,** 3565–3575 (2012).
47. Dolev, I. *et al.* Spike bursts increase amyloid-beta 40/42 ratio by inducing a presenilin-1 conformational change. *Nat. Neurosci.* **16,** 587–595 (2013).
48. Maritzen, T., Koo, S. J. & Haucke, V. Turning CALM into excitement: AP180 and CALM in endocytosis and disease. *Biol. Cell* **104,** 588–602 (2012).
49. Buggia-Prevot, V. *et al.* A function for EHD family proteins in unidirectional retrograde dendritic transport of BACE1 and Alzheimer's disease abeta production. *Cell Rep.* **5,** 1552–1563 (2013).
50. Udayar, V. *et al.* A Paired RNAi and RabGAP Overexpression Screen Identifies Rab11 as a Regulator of beta-Amyloid Production. *Cell Rep.* **5,** 1536–1551 (2013).
51. Yamakawa, H., Yagishita, S., Futai, E. & Ishiura, S. beta-Secretase inhibitor potency is decreased by aberrant beta-cleavage location of the 'Swedish mutant' amyloid precursor protein. *J. Biol. Chem.* **285,** 1634–1642 (2010).
52. Kamenetz, F. *et al.* APP processing and synaptic function. *Neuron* **37,** 925–937 (2003).
53. Tomita, T. *et al.* C terminus of presenilin is required for overproduction of amyloidogenic Abeta42 through stabilization and endoproteolysis of presenilin. *J. Neurosci.* **19,** 10627–10634 (1999).
54. Li, T., Ma, G., Cai, H., Price, D. L. & Wong, P. C. Nicastrin is required for assembly of presenilin/gamma-secretase complexes to mediate Notch signaling and for processing and trafficking of beta-amyloid precursor protein in mammals. *J. Neurosci.* **23,** 3272–3277 (2003).
55. Chiang, P. M., Fortna, R. R., Price, D. L., Li, T. & Wong, P. C. Specific domains in anterior pharynx-defective 1 determine its intramembrane interactions with nicastrin and presenilin. *Neurobiol. Aging* **33,** 277–285 (2012).
56. Herreman, A. *et al.* Total inactivation of gamma-secretase activity in presenilin-deficient embryonic stem cells. *Nat. Cell Biol.* **2,** 461–462 (2000).
57. Hayashi, I. *et al.* Single chain variable fragment against nicastrin inhibits the gamma-secretase activity. *J. Biol. Chem.* **284,** 27838–27847 (2009).
58. Ando, K. *et al.* Role of phosphorylation of Alzheimer's amyloid precursor protein during neuronal differentiation. *J. Neurosci.* **19,** 4421–4427 (1999).
59. Qi-Takahara, Y. *et al.* Longer forms of amyloid beta protein: implications for the mechanism of intramembrane cleavage by gamma-secretase. *J. Neurosci.* **25,** 436–445 (2005).
60. Takasugi, N. *et al.* BACE1 activity is modulated by cell-associated sphingosine-1-phosphate. *J. Neurosci.* **31,** 6850–6857 (2011).
61. Bretscher, M. S. & Lutter, R. A new method for detecting endocytosed proteins. *EMBO J.* **7,** 4087–4092 (1988).
62. Tomita, T. *et al.* The presenilin 2 mutation (N141I) linked to familial Alzheimer disease (Volga German families) increases the secretion of amyloid beta protein ending at the 42nd (or 43rd) residue. *Proc. Natl Acad. Sci. USA* **94,** 2025–2030 (1997).
63. Kakuda, N. *et al.* Equimolar production of amyloid beta-protein and amyloid precursor protein intracellular domain from beta-carboxyl-terminal fragment by gamma-secretase. *J. Biol. Chem.* **281,** 14776–14786 (2006).
64. Takahashi, Y. *et al.* Sulindac sulfide is a noncompetitive gamma-secretase inhibitor that preferentially reduces Abeta 42 generation. *J. Biol. Chem.* **278,** 18664–18670 (2003).

Acknowledgements

We are grateful to Drs T. Li, P.C. Wong (Johns Hopkins University), B. De Strooper (VIB Leuven), S. Yokoshima, T. Fukuyama, T. Kitamura (The University of Tokyo), M. Maki (Nagoya University), F. Barr (The University of Oxford) for valuable reagents, Takeda pharmaceutical company for Aβ ELISA, and our current and previous laboratory members for helpful discussions and technical assistance. This work was supported in part by grants-in-aid for Scientific Research (B, C) (for T.W. and Y.M.) and Young Scientists (S) (for T.T.) from the Japan Society for the Promotion of Science, Scientific Research on Innovative Areas for Foundation of Synapses and Neurocircuit Pathology (for T.I.) and Brain Environment (for T.T.) from the Ministry of Education, Culture, Sports, Science and Technology, Japan, by the Ministry of Health, Labor and Welfare of Japan (Comprehensive Research on Aging and Health) (for T.T.), by Core Research for Evolutional Science and Technology of JST (for T.T. and T.I.), by Takeda Science Foundation (for T.T.), by the Cell Science Research Foundation (for T.T.), by Cosmetology Research Foundation (for T.W.) and by a donation from Mr. Chuichi Imai (for T.T.).

Author contributions

Y.M. and T.T. designed the research. K.K., H.K. and Y.M. performed experiments. M.S. and T.W. generated *Picalm*$^{+/-}$ mice. K.K., Y.M., T.T. and T.I. wrote the paper.

Additional information

Supplementary Information accompanies this paper at http://www.nature.com/naturecommunications

Competing financial interests: The authors declare no competing financial interests.

Reprints and permission information is available online at http://npg.nature.com/reprintsandpermissions/

How to cite this article: Kanatsu, K. *et al.* Decreased CALM expression reduces Aβ42 to total Aβ ratio through clathrin-mediated endocytosis of γ-secretase. *Nat. Commun.* 5:3386 doi: 10.1038/ncomms4386 (2014).

Ohki et al. Molecular Neurodegeneration 2014, 9:7
http://www.molecularneurodegeneration.com/content/9/1/7

MOLECULAR NEURODEGENERATION

RESEARCH ARTICLE Open Access

Binding of longer Aβ to transmembrane domain 1 of presenilin 1 impacts on Aβ42 generation

Yu Ohki[1], Naoaki Shimada[2], Aya Tominaga[1], Satoko Osawa[1], Takuya Higo[2], Satoshi Yokoshima[2,3], Tohru Fukuyama[2,3], Taisuke Tomita[1,4*] and Takeshi Iwatsubo[1,4,5]

Abstract

Background: Amyloid-β peptide ending at 42nd residue (Aβ42) is believed as a pathogenic peptide for Alzheimer disease. Although γ-secretase is a responsible protease to generate Aβ through a processive cleavage, the proteolytic mechanism of γ-secretase at molecular level is poorly understood.

Results: We found that the transmembrane domain (TMD) 1 of presenilin (PS) 1, a catalytic subunit for the γ-secretase, as a key modulatory domain for Aβ42 production. Aβ42-lowering and -raising γ-secretase modulators (GSMs) directly targeted TMD1 of PS1 and affected its structure. A point mutation in TMD1 caused an aberrant secretion of longer Aβ species including Aβ45 that are the precursor of Aβ42. We further found that the helical surface of TMD1 is involved in the binding of Aβ45/48 and that the binding was altered by GSMs as well as TMD1 mutation.

Conclusions: Binding between PS1 TMD1 and longer Aβ is critical for Aβ42 production.

Keywords: Presenilin, Secretases, Alzheimer disease, Intramembrane proteolysis, γ-Secretase modulator

Background

Several lines of evidence suggest that the accumulation of amyloid-β peptide (Aβ), a major component of senile plaques, is a common pathological feature in Alzheimer disease (AD) [1]. Aβ is generated through sequential cleavage by β- and γ-secretases of amyloid-β precursor protein (APP). γ-Secretase primarily cleaves APP to produce a C-terminal stub of APP (APP-CTF). Then, scission of APP-CTF by γ-secretase results in generation of various forms of Aβ with different C-terminal lengths. Especially, Aβ ending at the 42nd residue (Aβ42), the most aggregable species, is initially and predominantly deposited in AD brains [2]. Moreover, familial AD-linked mutations in *Psen* (*Presenilin; PS*) *1*, *Psen2* or *APP* genes cause an increase in Aβ42 generation. Thus, Aβ42 is considered as the most pathogenic species causative for AD [3].

γ-Secretase is an intramembrane-cleaving protease complex composed of four membrane spanning proteins: PS, Nicastrin, Aph-1 and Pen-2 [4,5]. Extensive biochemical studies showed that the γ-secretase-mediated intramembrane cleavage of APP occurs in a processive manner [6]; APP-CTF is primarily cleaved at the ε-site located around the membrane-cytoplasm boundary to produce Aβ49 or Aβ48. Subsequently, these longer Aβ peptides are processed by stepwise cleavages to secrete shorter Aβ in two predominant production lines: Aβ49 is processed to Aβ43/40 via Aβ46 (Aβ40 production line), and Aβ48 is processed to Aβ42/38 via Aβ45 (Aβ42 production line). PS forms a channel-like catalytic pore structure within the membrane, and is endoproteolyzed to generate N- and C-terminal fragments (NTF and CTF, respectively) during the assembly of the protease-active complex [7,8].

Recently, small compounds that selectively regulate Aβ42 production without affecting ε-cleavage emerged, which are termed γ-secretase modulators (GSMs) [9]. We have shown that a potent Aβ42-lowering compound, GSM-1, directly targets the PS1 TMD1 [10]. Moreover, using substituted cysteine accessibility method (SCAM), we identified two different regions within TMD1 of PS1, i.e., a hydrophobic luminal region and a hydrophilic portion facing the catalytic site [11], that are differently

* Correspondence: taisuke@mol.f.u-tokyo.ac.jp
[1]Department of Neuropathology and Neuroscience, Graduate School of Pharmaceutical Sciences, The University of Tokyo, 7-3-1 Hongo, Bunkyo-ku, Tokyo 113-0033, Japan
Full list of author information is available at the end of the article

involved in the action of GSM-1 [10]. However, the precise molecular mechanism whereby γ-secretase generates Aβ42, as well as the role of TMD1 in Aβ42 production, remains elusive. In this study, we identified TMD1 of PS1 as a regulatory domain for the processive cleavage of the Aβ42 production line.

Results

Fenofibrate directly targets the N-terminal fragment of presenilin 1

Fen-B [12] is a derivative of the Aβ42-raising GSM, fenofibrate [13], coupled to a biotin moiety. Previous report showed that Fen-B directly targeted APP-CTF by photo-crosslinking using recombinant proteins or microsomes under overexpression conditions. However, the possibility of a nonspecific binding of fenofibrate to high concentrations of APP in an artificial condition was not excluded [14,15]. We performed a photoaffinity labeling experiment with Fen-B using microsomes prepared from brains of wild-type mice. We found that endogenous PS1 NTF, but neither of other γ-secretase components (i.e., PS1 CTF, Nicastrin, Aph-1 and Pen-2) nor APP-CTF, was specifically precipitated (Figure 1A). In addition, we detected a biotinylated band of ~30 kDa, corresponding to the molecular weight of PS1 NTF, in the fraction incubated with Fen-B. To further confirm the specificity of labeling of PS1 NTF by Fen-B, membrane fractions of fibroblasts from *Psen1*$^{-/-}$/*Psen2*$^{-/-}$ double knockout mice (DKO) [16] with or without overexpression of His-tagged PS1 [17] were subjected to PAL. Biotinylated PS1 NTF was specifically precipitated, indicating that PS1 NTF is targeted by Fen-B (Figure 1B). Finally, a specific binding of Fen-B to SPP, another aspartic intramembranous cleaving protease, which shared homology with PS [18], was also observed (Figure 1C). Taken together, we concluded that the *bona fide* molecular target of fenofibrate, in the context of modulation of intramembrane cleavage, are PS1 and SPP, i.e., the enzyme moieties.

To narrow down the fenofibrate binding site within PS1 NTF, we employed the limited digestion approach by inserting a thrombin substrate sequence into PS1 [10]. γ-Secretase containing PS1-Th1 mutant, in which thrombin cleavable sequence was inserted between D110 and G111 in the hydrophilic loop 1, harbored γ-secretase activity and was sensitive to fenofibrate (Figure 2A). Eight kDa N-terminal fragment of PS1 NTF generated by thrombin cleavage of PS1-Th1 after Fen-B

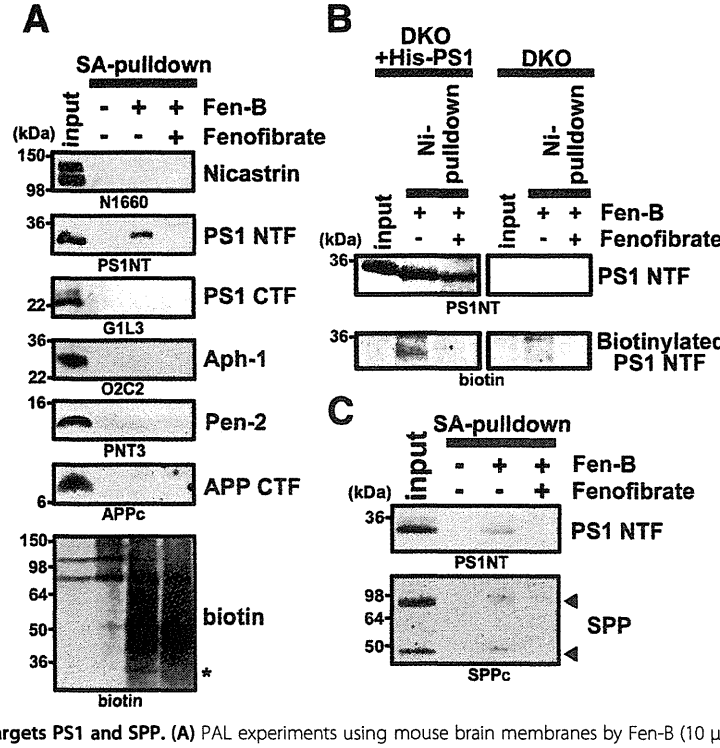

Figure 1 Fen-B directly targets PS1 and SPP. (A) PAL experiments using mouse brain membranes by Fen-B (10 μM). This labeling was competed by treatment with fenofibrate (200 μM). Note that only PS1 NTF was specifically labeled by Fen-B. Anti-biotin antibody also reacted with a band with ~30 kDa corresponding to PS1 NTF (an asterisk). **(B)** Fen-B labeling experiment for the DKO cells expressing His-tagged PS1. After PAL, His-tagged PS1 was purified with Ni^{2+}-affinity column and analyzed by immunoblotting. **(C)** Fen-B also bound endogenous monomeric as well as dimeric SPP (arrows) in CHO cell membranes.

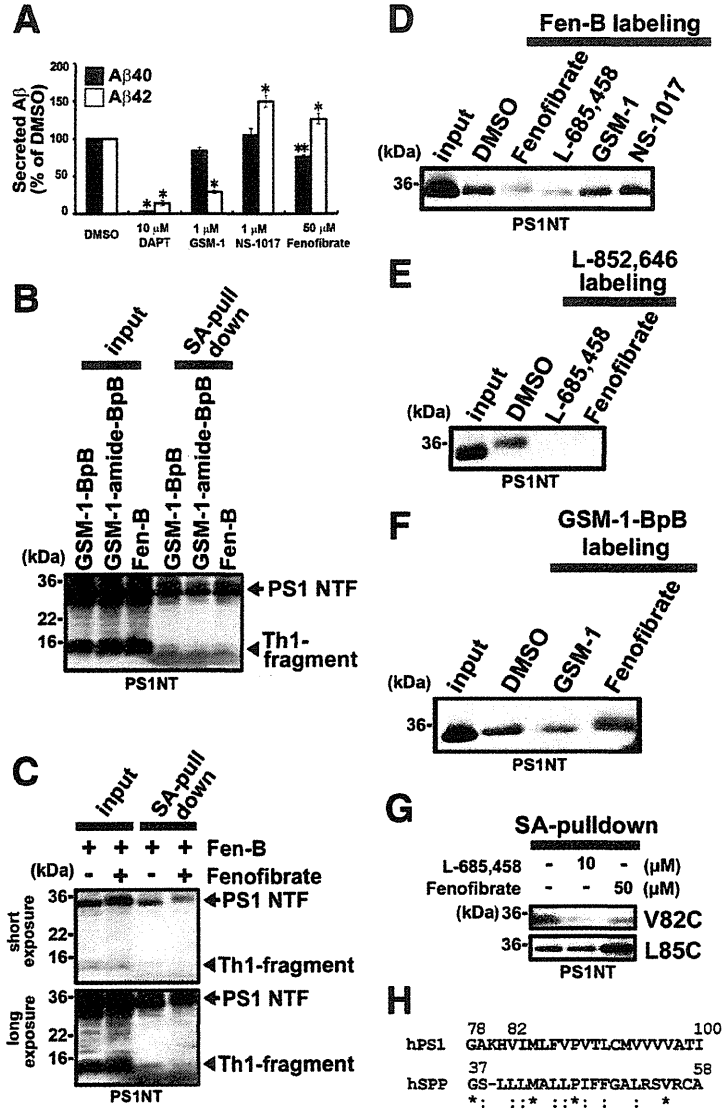

Figure 2 Cytosolic side of TMD1 forms a fenofibrate binding pocket. (A) Sensitivity of PS1-Th1 for GSMs. Effect of DAPT (10 μM), GSM-1 (1 μM), NS-1017 (1 μM) and fenofibrate (50 μM) on secreted Aβ from wild-type PS1 containing γ-secretase using DKO cells stably expressing APPNL (n = 3, mean ± SD, *p < 0.01, **p < 0.05 at Student's t test). **(B)** Thrombin digestion experiments were performed after PAL by GSM-1-BpB (1 μM), GSM-1-amide-BpB (1 μM) and Fen-B (10 μM). Note that cleaved Th1-fragment (arrowhead) was precipitated and detected by anti-PS1 NTF antibody. **(C)** Labeling competition analysis of Fen-B (10 μM) in the presence of fenofibrate (100 μM) using PS1-Th1 microsomes. Upper and lower panels show short and long exposures, respectively. **(D)** Labeling competition analyses were performed with fenofibrate (100 μM), L-685,458 (10 μM), GSM-1 (100 μM) and NS-1017 (100 μM) for the labeling of PS1 NTF by Fen-B (10 μM). **(E)** Labeling competition experiment with L-685,458 (10 μM) and fenofibrate (100 μM) for the labeling of PS1 NTF by L-852,646 (100 nM). **(F)** Labeling competition analysis by GSM-1-BpB (1 μM) in the presence of GSM-1 (100 μM) or fenofibrate (100 μM) using CHO cell microsomes. **(G)** SCAM analyses of microsomes from DKO cells expressing single-Cys mt PS1 containing one Cys at 82 or 85 positions in the presence or absence of indicated compounds. Note that the labeling of V82C was decreased and of L85C was increased by preincubation with fenofibrate. **(H)** Alignment of amino acid residues of PS1 TMD1 (78th to 100th residues) and 37th to 58th residues of SPP, which includes predicted TMD1 (32nd to 54th residues [19]). Asterisks and colons indicate conserved and similar amino acids, respectively.

crosslinking was specifically precipitated in a similar fashion to that by phenylpiperidine-type photoprobes, suggesting that Fen-B also targets to the most N-terminal region of PS1, including TMD1 (Figure 2B and C). We showed that the cytosolic side of TMD1 participates in the catalytic hydrophilic pore [7,11]. To analyze the relationship between the fenofibrate binding site and the catalytic site within TMD1, we employed the cross-

competition analysis in Fen-B labeling using different classes of compounds. Labeling of PS1 NTF by Fen-B was diminished by L-685,458, that directly targets the cytosolic side of TMD1 (Figure 2D) [11]. Consistent with this, labeling of PS1 NTF by L-852,646, an L-685,458-based photoprobe, was inhibited by fenofibrate (Figure 2E). In contrast, neither GSM-1 nor NS-1017, which targets the luminal region of TMD1, affected the binding of Fen-B (Figure 2D). Moreover, biotinylation of PS1 NTF by GSM-1-BpB was hardly affected by fenofibrate (Figure 2F), suggesting that the binding site of fenofibrate is distinct from that of GSM-1 within TMD1. We then performed a labeling competition experiment in SCAM [7,11], the latter being a biochemical method to deduce the structure of the membrane protein by position-specific biotinylation and to identify the targeting site of the compound of interest. Preincubation of fenofibrate decreased the biotinylation at Val82, supporting the notion that fenofibrate targets the catalytic site. In contrast, labeling of Leu85 was increased, indicating that fenofibrate evokes a conformational change of the catalytic site in TMD1 (Figure 2G). Intriguingly, Gly37 to Ala58 of SPP, which encompassed the predicted SPP TMD1 (Ile32 to Ser54) [19], showed a substantial homology to primary sequence of N-terminal region of PS1 TMD1 (i.e., Gly78 to Ile100) (Figure 2H), suggesting the possibility that fenofibrate targets to the predicted SPP TMD1. Taken together with the results of chemical biological experiments, the binding site of fenofibrate was estimated to locate around Val82 in TMD1, leading to the conformational change of the catalytic site of γ-secretase.

Intermediate longer A was secreted by TMD1 mutant PS1

This finding prompted us to hypothesize that TMD1 is potentially involved in the regulation of the processivity of γ-secretase to generate Aβ42. To address this issue, we screened single cysteine (single-Cys) mutants of TMD1 in cysteine-less PS1 used in SCAM. While cysteine-less PS1 increased Aβ42(43)/Aβ40 ratio compared to that of wild-type PS1-expressing cells, some single-Cys mutants showed further augmentation in Aβ42(43)/Aβ40 ratio (Figure 3A). Among these mutants, P88C mutant showed a dramatic increase in the Aβ42 (43)/Aβ40 ratio. To further analyze the functional significance of Pro88 in the processive cleavage, we analyzed two PS1 mutants, P88C and P88L. Surprisingly, P88L mutation caused an increase in the Aβ42(43)/Aβ40 ratio, to a level higher than that with L166P mutant PS1 (Figure 3C and D), one of the most potent pathogenic PS1 mutations [20]. In addition, P88L mutant elicited secretion of the intermediate, longer form of Aβ, i.e. Aβ45

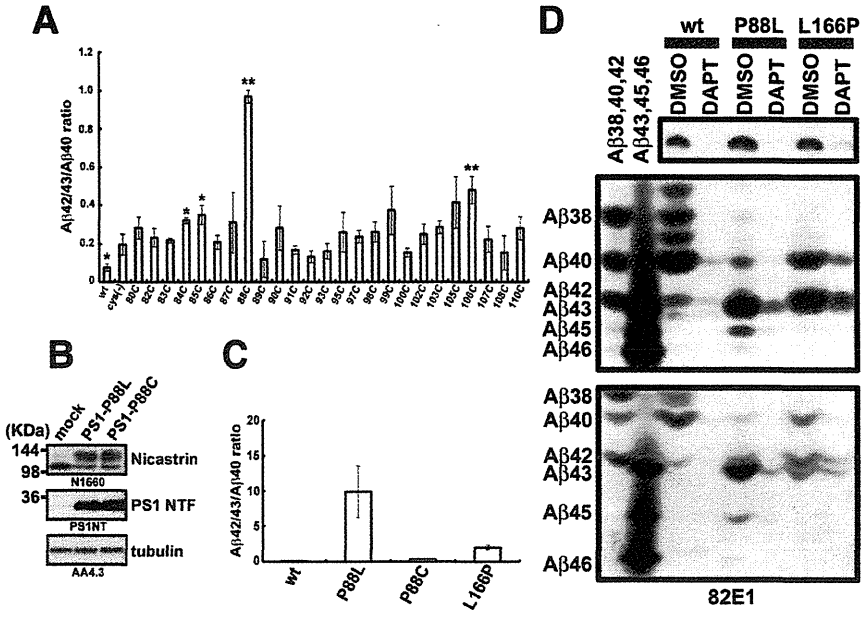

Figure 3 Pro88 is the critical amino acid residue for the determination of length of secreted Aβ. (A) Aβ42(43)/Aβ40 ratio in secreted Aβ from DKO cells expressing Single-Cys mt PS1. Conditioned media were analyzed by ELISA (n = 3, mean ± SD, *p < 0.05, **p < 0.01 (Compared with Cys-less) at Student's t test). **(B)** Immunoblotting analysis of DKO cell lysate expressing PS1 mutant carrying P88C or P88L by indicated antibodies. **(C)** Aβ42(43)/Aβ40 ratio in secreted Aβ from DKO cells in **(B)** measured by ELISA (n = 3, mean ± SD). **(D)** Urea-SDS gel analysis for secreted Aβ from DKO cells expressing wild-type PS1, PS1 with P88L or PS1 with L166P mutation. Conditioned media of cells treated with 10 μM DAPT were also analyzed. Two types of Urea-SDS gels were used to obtain better resolution in the detection of longer Aβ peptides (i.e., Aβ45 and Aβ46).

and Aβ46, but neither in the wild-type nor L166P mutant PS1 (Figure 3D). These data strongly implicated TMD1 in the regulation of the C-terminal length of Aβ.

GSMs and P88L mutation affected the interaction between TMD1 and longer Aβ species

Our unexpected observation of an abnormal secretion of longer Aβ45 from cells expressing P88L mutant PS1 prompted us to further investigate the functional role of TMD1 during the enzymatic process, especially the processive cleavage. Notably, previous reports indicated that a region between Val82 to Ser132 encompassing TMD1 directly participates in the interaction with γ-secretase substrates (i.e., APP-CTF) *in vitro* [21-23]. Moreover, Aβ46 has been shown to accumulate by DAPT, which inhibits processive cleavage, and to be coimmunoprecipitated with PS1 [23,24]. These results implied the possibility that TMD1 directly recognizes the longer Aβ species during the processive cleavage of γ-secretase. To test this idea, we performed *in vitro* binding assays of various longer Aβ species with purified GST, GST-PS1$_{1\text{-}110}$ and GST-TM1mt$_{1\text{-}110}$, the latter harboring the TMD1 sequence (i.e., Val82 to Ile100) replaced with a TMD of an unrelated membrane protein, CLAC-P [10,25] (Figure 4A and B). Replacement of TMD1 of PS1 with CLAC-P sequence abolished the γ-secretase activity [17] as well as binding of GSM-1-BpB *in vitro* [10] (Figure 4C), indicating chimeric PS1 with CLAC sequence has a distinct property. Then synthetic Aβ peptides were coincubated with recombinant proteins and pulled down by glutathione sepharose (Figure 4D). In this condition, we detected specific binding of recombinant C99-FLAG to GST-PS1$_{1\text{-}110}$, as previously reported by Annaert et al [21]. In addition, we detected binding of all synthetic longer Aβ peptides (Aβ49, Aβ48, Aβ46, Aβ45, Aβ43) with GST-PS1$_{1\text{-}110}$, suggesting that TMD1 of PS1 directly binds to longer Aβ peptides, and that the cytoplasmic domain of APP is not involved in this binding. Unexpectedly, GST-TM1mt$_{1\text{-}110}$ was capable of interacting with C99-FLAG as well as with peptides belonging to the Aβ40 production line (Aβ49, Aβ46 and Aβ43). However, the binding of Aβ species of the Aβ42 production line (i.e., Aβ48 and Aβ45) was significantly reduced by swapping the TMD1 sequence (Figure 4D). We further analyzed the effect of TMD1-targeting GSMs as well as P88L mutation on the binding of Aβ45 and Aβ48 to TMD1. Intriguingly, GSM-1 augmented the interaction of TMD1 with Aβ45 as well as Aβ48, whereas it was reduced by fenofibrate (Figure 4E). In addition, introduction of P88L mutation in GST PS1$_{1\text{-}110}$ decreased the pull down of Aβ45 (Figure 4F). Finally, we observed a specific binding of Aβ48 with native PS1

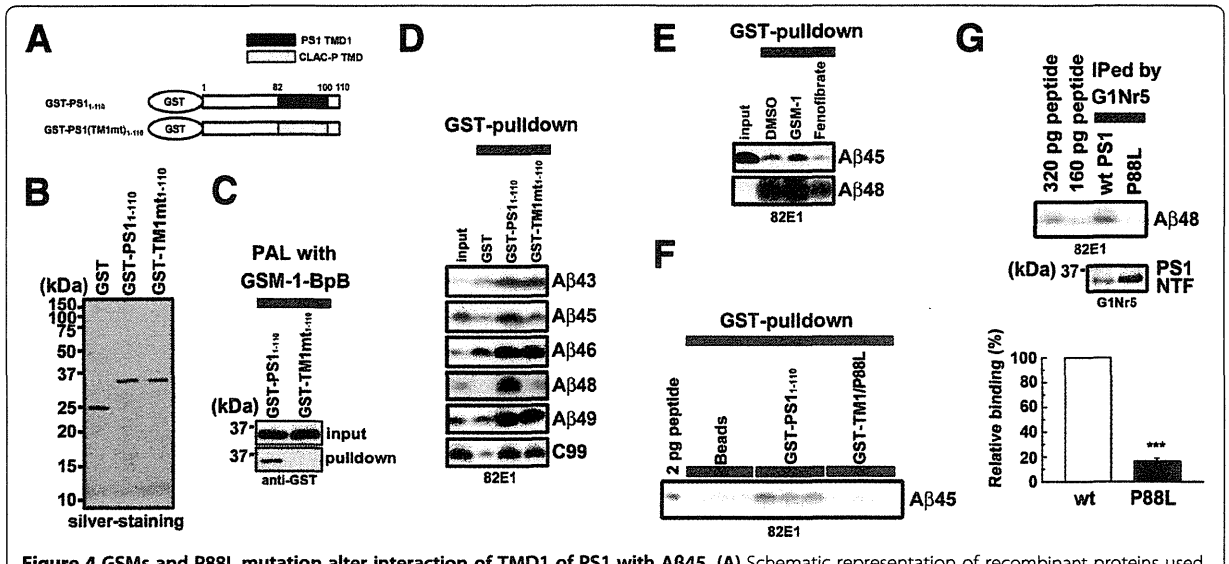

Figure 4 GSMs and P88L mutation alter interaction of TMD1 of PS1 with Aβ45. (A) Schematic representation of recombinant proteins used in this study. **(B)** GST and GST-fused recombinant proteins were purified by glutathione sepharose and/or Mono Q column. The purity of purified recombinant proteins was confirmed by silver staining. **(C)** GSM-1-BpB (4 nM) labeling experiment for GST-PS1$_{1\text{-}110}$ and TMD1 swapping mutant, GST-TM1mt$_{1\text{-}110}$ (0.19 μg). Samples were preincubated with photoprobes on ice for 10 min, and then irradiated for 60 min. **(D)** Pull down assay of GST-fused recombinant proteins mixed with longer Aβ (Aβ43/45/46/48/49) (1 nM). After incubation with glutathione sepharose, all samples were washed and subjected to immunoblot. **(E)** The effects of GSM-1 (25 μM) or fenofibrate (100 μM) on the interaction of GST-PS1$_{1\text{-}110}$ with longer Aβ peptides. Recombinant proteins were preincubated with GSMs and then incubated with longer Aβ peptides. Protein complexes were pulled down by glutathione sepharose and analyzed by immunoblot. **(F)** The effect of P88L mutation on the binding of Aβ45 peptide to GST-PS1$_{1\text{-}110}$. **(G)** Binding of Aβ48 peptide to native PS1 protein expressed in mammalian cells. Densitometric analysis of relative levels of the bound Aβ48 was shown at the below (n = 3, mean ± SD, ***p <0.001 at Student's t test).

protein expressed in the mammalian cells, and this interaction was almost diminished by the P88L mutation (Figure 4G). We did not observe specific binding of Aβ45 with PS1 holoprotein expressed in mammalian cells, presumably due to weak binding of Aβ45 to PS1 protein. Nevertheless, these data suggest that the processivity of the γ-secretase for Aβ42 production is defined by the tenacity of interaction between TMD1 and longer Aβ, which may determine the retention of the substrate in the catalytic site. Collectively, we uncovered the significant function of TMD1 of PS1 as a binding site for the longer Aβ species, especially Aβ45 and Aβ48, during the processive cleavage of the Aβ42 production line, and the effects of GSMs on Aβ42 production by changing the affinity between TMD1 and the longer Aβ peptides.

Discussion

Understanding the molecular mechanism of the processive cleavage by γ-secretase is critical to the development of effective GSMs. We previously reported that phenylpiperidine-type GSMs are bound to TMD1 of PS1 [10]. Here, we further showed that fenofibrate, an Aβ42-raising GSM, also directly targets TMD1, while Fen-B was reported as APP-targeting photoprobe [12]. Recently, some papers reported that large amount of Aβ42 or C99 forms aggregates that cause non-specific binding to GSMs [14,15]. Therefore, we have used brain microsomes obtained from wild-type mouse for the photocrosslinking experiment.

Scissile bonds for processive cleavage by γ-secretase have hypothetically been mapped on different surfaces in the α-helical model of APP TMD [26]. This raises the possibility that the distinct processive cleavages by γ-secretase, i.e., those leading to production of Aβ49-46-43-40 or Aβ48-45-42-38, are determined by the recognition of one or the other of the specific helical surfaces. However, the domain on γ-secretase that recognizes the helical surface on the substrate is yet to be identified. It has previously been suggested that TMD1 of PS1 is involved in the binding of APP-CTF, a direct substrate of γ-secretase [21,22]. Here we found that longer Aβ peptides that are generated as intermediate products in the Aβ42 production line (i.e., Aβ45 and Aβ48), which also are direct substrates for the processive cleavage, retain the capacity to interact with TMD1 of PS1. It is highly likely that the "gripping tenacity" of the substrate binding site facing the catalytic pore would determine the processivity of Aβ48 and Aβ45 on the Aβ42 production line, which can be modulated by small compounds. Consistently, Okochi et al. have recently reported that Aβ42 is bound to the γ-secretase complex [27] and the binding was modulated by GSMs, although they have not identified the binding site of Aβ within the enzyme complex. Thus, we propose that TMD1 of PS1 functions as a binding site of longer Aβ species for γ-secretase during the processive cleavage, which specifically determines the efficiency of the processive cleavage of the Aβ42 production line. Structural analyses suggested that the catalytic cavities of rhomboid protease [28], another intramembrane-cleaving enzyme, or those of FlaK [29] and PSH [30], archaeal GxGD proteases, are unable to accommodate all the amino acid residues of the transmembrane sequence of the substrates. This suggests that a major part of the TMD of substrates remains within the membrane and is gripped by enzymes to incorporate the cleavage site into the intramembrane catalytic site during proteolysis. While the precise structure of human PS1 still remains unclear, our SCAM results on PS1 [11], as well as the recently reported x-ray crystal structure of PSH [30], the latter being composed of 9-transmembrane domains similarly to human PS1, altogether suggested that TMD1 locates in proximity to the catalytic aspartate in TMD7. The results of these structural analyses also support our notion that TMD1 functions as a substrate binding domain during the processive cleavage by γ-secretase.

TMD1 of PS1 bound not only to longer Aβ peptides of the Aβ42 production line, but to those of Aβ40 line (Figure 4D). P88L mutation in TMD1 of PS1 caused an increased secretion of not only Aβ45, but also Aβ43 and Aβ46 (Figure 3F), suggesting that the interaction between TMD1 and longer Aβ species is also critical for the processivity in the Aβ40 production line. Intriguingly, swapping TMD1 sequence of PS1 with that of CLAC-P, an unrelated membrane protein, did not affect the binding of Aβ43, Aβ46 and Aβ49 peptides. In the helical net diagram, similar side chains at the luminal side of PS1 TMD1 and CLAC-P TMD comprised an interface on the α-helical model only in one side (Figure 5A and B) [31]. Thus, one helical surface of TMD1 is involved in the binding of longer Aβ species in the Aβ40 production line, whereas the other surface specifically interacts with those in the Aβ42 production line in the PSH-based PS1 model (Figure 5C). Pharmacological and chemical biological studies suggest that the substrate enters the catalytic site via the initial substrate binding site, in which TMD2, 6 and 9 are involved [17]. Especially, TMD6 and 9 have been implicated in the lateral entry of the substrate from the crystal structure of PSH [30]. However, helical peptide-type GSIs that target the initial substrate binding site equally inhibited the production of Aβ40 or Aβ42 [32,33]. Thus, we hypothesize that C99 or longer Aβ is gripped by TMD1 after the lateral entry (Figure 5D). Structural model also suggested that residues related to the Aβ42 production line in the luminal side of TMD1 are located on the surface of PS1 polypeptide, which might be targeted by GSM-1 [10]. In fact, several side chain interactions have been identified in

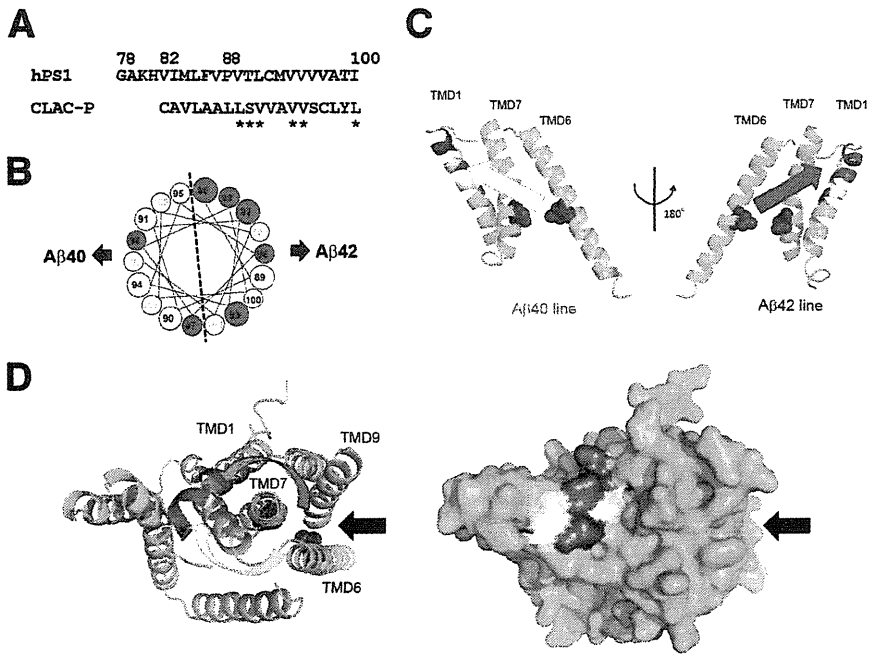

Figure 5 Hypothetical model of the role of PS1 TMD1 in Aβ42 generation. (A and B) Alignment of amino acid residues of the human PS1 TMD1 and CLAC-P. In the swap mutant PS1, 82nd to 100th residues were replaced with CLAC-P TMD. Residues with similar side chains are labeled with asterisks in **(A)** and as yellow circles in **(B). (C)** Modified structural model of PS1 based on PSH structure kindly provided from Dr. Y. Shi [30]. Side views of the ribbon model of TMD1, 6 and 7 generated by Pymol are shown. Yellow and purple residues correspond to those in **(B)**. Possible approaches to the catalytic aspartates (red spheres) for Aβ40 and Aβ42 production lines are shown by yellow and purple arrows, respectively. TMD1 grips the substrate to prevent its liberation during the processive cleavage. Helix-helix interaction of longer Aβ with TMD1 determines the major production line (i.e., Aβ40 or Aβ42) of processive cleavage. **(D)** Top views of the whole PS1 model (left; ribbon diagram; right, surface model) generated by Pymol are shown. Putative substrate entry site [30] is shown as black arrows.

TMD1 and the neighboring TMDs [30]. However, we have previously suggested a piston-like vertical movement of TMD1 by SCAM [34], supporting our view that dynamic conformational changes would take place during the catalytic reaction. Intriguingly, the reason why the efficiency of Aβ42 production is always lower than that of Aβ40 in any cell types [35] has been unknown. Considering the positions of the first ε-cleavage sites located on the opposite sides of the helical surfaces predicted for the Aβ40 and Aβ42 production lines, it is tempting to speculate that an approach of the substrate from an unfavored direction (pink arrow, Figure 5) to the catalytic site in terms of stereochemistry might explain the lower efficiency of cleavage in the Aβ42 production line (Figure 5C and D). However, the other TMDs might be also involved in the recognition of Aβ42, and GSMs could allosterically affect these other regions including initial substrate binding site in PS1. Biochemical analysis to identify the other binding domain for longer Aβ peptides belonging to the Aβ40 production line would provide further molecular insights regarding the mechanism of action of GSMs. Also structural analysis of mammalian PS1 carrying P88L mutation might unveil further mechanistic role of TMD1 in the trimming process by γ-secretase. In sum, we revealed that TMD1, a previously identified target region of GSMs, participates in the Aβ42 generation as a binding site that docks longer Aβ species as intermediate substrates for γ-secretase. Our observations may shed light on the molecular mechanism of the processive cleavage by γ-secretase, contributing to the development of potent and selective Aβ42-lowering compounds for AD.

Conclusions

Fenofibrate directly bound to TMD1 of PS1 to induce the conformational changes in the catalytic site of the γ-secretase. P88L mutation in TMD1 caused an aberrant secretion of longer Aβ polypeptides (i.e., Aβ45 or Aβ46), indicating that TMD1 is involved in the regulation of C-terminal length of Aβ. Finally, we found that TMD1 contains a binding site for the longer Aβ species, and GSMs affect Aβ42 production by changing the affinity between TMD1 and longer Aβ. Our results suggest that TMD1 functions as a substrate binding domain during the processive cleavage by γ-secretase.

Methods

Compounds, peptides and antibodies

GSM-1, GSM-1-BpB, NS-1017, GSM-1-amide-BpB, Fen-B and DAPT were synthesized as described [10,12,36]. L-685,458 and fenofibrate were purchased from Bachem and SIGMA, respectively. L-852,646 [37] was kindly provided from Dr. Y. Li (Sloan-Kettering Cancer Center). Synthetic longer Aβ peptides (i.e., β-amyloid (1-43, #23573), (1-45, #61956-01), (1-46, #62076-01), (1-48, #61965-01), (1-49, #61963-01) were purchased from Anaspec. Aβ (1-40) (#4307-v) and Aβ (1-42) (#4349-v) peptides were purchased from Peptide institute. The rabbit polyclonal antibodies anti-PS1 NTF (G1Nr5), anti-PS1 CTF (G1L3) and anti-Pen-2 (PNT3) were raised as described [38-40]. Anti-PS1 NTF (PS1NT) [41] and anti-SPP (SPPc) [42] were kindly gifted from Drs. G. Thinakaran (The University of Chicago) and T. Golde (University of Florida). Anti-nicastrin N1660 (SIGMA), anti-APP CTF (Immuno-Biological Laboratories), anti-Aph-1aL O2C2 (Covance), anti-human Aβ 82E1 (Immuno-Biological Laboratories) and anti-biotin (Bethyl) were purchased from indicated vendors. The monoclonal antibody anti-α-tubulin AA4.3 developed by Dr. C. Walsh was obtained from the Developmental Studies Hybridoma Bank developed under the auspices of the NICHD, National Institutes of Health, and maintained by The University of Iowa, Department of Biology, Iowa City, IA.

Plasmid construction, cell culture manipulation and cell based assay

cDNAs encoding PS1 and APP carrying Swedish mutation (APPNL) were inserted into pMXs-puro [43]. cDNAs encoding mutant PS1 were generated by long PCR-based QuikChange™ strategy (Stratagene). To produce recombinant proteins, cDNAs encoding PS1 were cloned into pGEX-6P-1 vector (GE healthcare) [10]. Maintenance of cultured cells, transfection, retroviral infection, two-site enzyme-linked immunosorbent assay (ELISA), or immunoblotting using Urea/SDS-PAGE gel system as described [10,39,44,45].

Photoaffinity labeling and SCAM experiments

Preparation of samples for photoaffinity labeling experiments [46] was performed as follows. Brains of C57J/B6 mouse (3-5 month age) or cultured cells were homogenized with homogenize buffer (20 mM HEPES (pH 7.0), 140 mM KCl, 250 mM sucrose, 0.5 mM diisopropyl fluorophosphate, 0.5 mM phenylmethylsulfonyl fluoride, 1 μg/ml tosyllysine chloromethyl ketone, 1 μg/ml antipain, 1 μg/ml leupeptin, 10 μg/ml phosphoramidon, 5 mM EDTA, 1 mM EGTA) using Potter-Elvehjem Tissue Grinder (Wheaton), and membrane fractions were collected by ultracentrifugation at 100,000 × g (Beckman) [10]. PAL experiments utilizing avidin-biotin catch principle [47] and thrombin digestion experiments after PAL were performed as previously described [10]. Briefly, after resuspension of the microsome in the homogenize buffer by 25G needle with syringe, protein content was measured by BCA assay (Thermo Fisher Scientific). 1 mL of microsome-containing solution (1 mg/ml protein) was preincubated with compounds for 30 min on ice. Then photoprobes were added and incubated for 10 min on ice under the dark condition. UV irradiation (352 nm) was performed on ice for 1 hr with a UV lamp (Model XX-15BLB, UVP). The approximate distance from UV lamp to the samples was 10 cm. The biotinylated proteins were precipitated by streptavidin sepharose (GE healthcare) in 1% SDS containing homogenization buffer. For SCAM, all methanethiosulfonate reagents (Toronto Research Chemicals) were dissolved in dimethyl sulfoxide at 200 mM prior to use or stored at 80 degree until use. The methods for SCAM and competition experiments using biotinylaminoethyl methanethiosulfonate have been described in detail before [10,11]. Briefly, stable DKO cells expressing cysteine mutant PS1 were grown on two 15-cm dishes per single analysis. Cells were scraped in PBS and resuspended in 2 ml of SCAM homogenization buffer (10 mM HEPES (pH 7.4), 150 mM NaCl, 10% glycerol, Complete protease inhibitor cocktail (Roche Biochemicals)). Cells were disrupted by a Polytron homogenizer (Hitachi), and nuclei and large cell debris were pelleted by centrifugation at 1,500 × g for 10 min. The postnuclear supernatants were centrifuged, and the resultant microsomal pellets were resuspended in 0.2 ml of PBS in a syringe, and 0.1 mM biotinylaminoethyl methanethiosulfonate was added to this fraction. After 30 min incubation at 4 degree, microsomes were centrifuged twice to wash out. The resultant pellets resuspended in 1% SDS/PBS were incubated with the streptavidin sepharose overnight and analyzed as in the intact cell biotinylation experiment. In PAL or SCAM experiments, we loaded 1.5 and 20% of samples as "input" and "bound", respectively, in all immunoblot analyses.

Protein purification and binding assay

GST-fusion recombinant proteins were expressed in *E. Coli* (BL21 DE3) (Novagen) and purified by two step procedures using glutathione sepharose and mono Q columns (GE Healthcare) as manufacturer's instruction. All recombinant proteins were finally diluted with recombinant protein preparation buffer (10 mM HEPES (pH 7.4), 150 mM NaCl, 0.25% CHAPSO). C99-FLAG was purified from Sf9 cells infected with recombinant baculovirus encoding C99-FLAG and diluted at 1 μg/ml in recombinant protein preparation buffer. To perform binding assay, 0.5 μg of GST-fusion recombinant

proteins were mixed at 1 μg of C99-FLAG, 1 (for Aβ43, Aβ45, Aβ46, Aβ48 and Aβ49) or 10 (for Aβ40 and Aβ42) nM of synthetic Aβ in 1 ml of recombinant protein preparation buffer, and incubated at 4 degree overnight. After addition of glutathione sepharose, samples were then washed with the buffer and precipitates were eluted by boiling in sample buffer. For binding assay using native PS1 protein, PS1 or P88L mutant PS1 was expressed in DKO cells and solubilized in 10 mM HEPES buffer containing 1% CHAPSO. After addition of 2 ng of Aβ48 peptide, the solubilized fraction was incubated with anti-PS1 antibody G1Nr5 at 4 degree overnight. PS1-Aβ48 complex was then immunoprecipitated using Protein G sepharose 4 Fast Flow (GE Healthcare). Subsequently eluates (i.e., proteins bound to GST-fusion recombinant proteins or native PS1 proteins) were analyzed by immunoblotting. We loaded 0.75 and 20% of samples as "input" and "bound", respectively, in immunoblot of all pull down assay unless the amount of loaded proteins was otherwise indicated.

Abbreviations

AD: Alzheimer disease; CTF: Carboxyl-terminal fragment; DKO: *Psen1/Psen2* double knockout mouse immortalized fibroblasts; GSM: γ-secretase modulator; NTF: Amino-terminal fragment; mt: Mutant; PS: Presenilin; SCAM: Substituted cysteine accessibility method; TMD: Transmembrane domain.

Competing interests

The authors declare that they have no competing interests.

Authors' contributions

YO and TT designed the research. YO, AT, SO and TT performed biochemical experiments. NS, TH, SY and TF synthesized the compounds. YO, TT and TI wrote the paper. All authors read and approved the final manuscript.

Acknowledgements

The authors are grateful for G. Thinakaran (The University of Chicago), T. Golde (University of Florida), B. De Strooper (VIB Leuven), Y. Li (Sloan-Kettering Cancer Center), and T. Kitamura (The University of Tokyo), S. Funamoto and Y. Ihara (Doshisha University), and Takeda pharmaceutical company for Aβ ELISA for valuable reagents, and our current and previous laboratory members for helpful discussions and technical assistance. This work was supported in part by grants-in-aid for Young Scientists (S) from the Japan Society for the Promotion of Science (JSPS) (T.T.), Scientific Research on Innovative Areas for Foundation of Synapses and Neurocircuit Pathology (for T.I.) and Brain Environment (for T.T.) from the Ministry of Education, Culture, Sports, Science and Technology, Japan, by the Ministry of Health, Labor and Welfare of Japan (Comprehensive Research on Aging and Health) (for T. T.), by Targeted Proteins Research Program of the Japan Science and Technology Corporation (JST) (for T.T., T.I.), by Core Research for Evolutional Science and Technology of JST (for T.T., T.I.) and by a donation from Mr. Chuichi Imai (for T.T.). Y.O. and T.H. are research fellows of JSPS.

Author details

[1]Department of Neuropathology and Neuroscience, Graduate School of Pharmaceutical Sciences, The University of Tokyo, 7-3-1 Hongo, Bunkyo-ku, Tokyo 113-0033, Japan. [2]Department of Synthetic Natural Chemistry, Graduate School of Pharmaceutical Sciences, The University of Tokyo, Bunkyo-ku, Tokyo 113-0033, Japan. [3]Laboratory of Natural Products Chemistry, Graduate School of Pharmaceutical Sciences, Nagoya University, Nagoya 464-8601, Japan. [4]Core Research for Evolutional Science and Technology, Japan Science and Technology Agency, Bunkyo-ku, Tokyo 113-0033, Japan. [5]Department of Neuropathology, Graduate School of Medicine, The University of Tokyo, Bunkyo-ku, Tokyo 113-0033, Japan.

Received: 8 November 2013 Accepted: 10 January 2014
Published: 13 January 2014

References

1. Holtzman DM, Morris JC, Goate AM: **Alzheimer's disease: the challenge of the second century.** *Sci Transl Med* 2011, **3**:77sr71.
2. Iwatsubo T, Odaka A, Suzuki N, Mizusawa H, Nukina N, Ihara Y: **Visualization of A beta 42(43) and A beta 40 in senile plaques with end-specific A beta monoclonals: evidence that an initially deposited species is A beta 42(43).** *Neuron* 1994, **13**:45–53.
3. De Strooper B, Annaert W: **Novel research horizons for presenilins and gamma-secretases in cell biology and disease.** *Annu Rev Cell Dev Biol* 2010, **26**:235–260.
4. Takasugi N, Tomita T, Hayashi I, Tsuruoka M, Niimura M, Takahashi Y, Thinakaran G, Iwatsubo T: **The role of presenilin cofactors in the gamma-secretase complex.** *Nature* 2003, **422**:438–441.
5. Tomita T, Iwatsubo T: **Structural biology of presenilins and signal peptide peptidases.** *J Biol Chem* 2013, **288**:14673–14680.
6. Takami M, Nagashima Y, Sano Y, Ishihara S, Morishima-Kawashima M, Funamoto S, Ihara Y: **gamma-Secretase: successive tripeptide and tetrapeptide release from the transmembrane domain of beta-carboxyl terminal fragment.** *J Neurosci* 2009, **29**:13042–13052.
7. Sato C, Morohashi Y, Tomita T, Iwatsubo T: **Structure of the catalytic pore of gamma-secretase probed by the accessibility of substituted cysteines.** *J Neurosci* 2006, **26**:12081–12088.
8. Morohashi Y, Tomita T: **Protein trafficking and maturation regulate intramembrane proteolysis.** *Biochimica et biophysica acta* 1828, **2013**:2855–2861.
9. Tomita T: **Secretase inhibitors and modulators for Alzheimer's disease treatment.** *Expert Rev Neurother* 2009, **9**:661–679.
10. Ohki Y, Higo T, Uemura K, Shimada N, Osawa S, Berezovska O, Yokoshima S, Fukuyama T, Tomita T, Iwatsubo T: **Phenylpiperidine-type gamma-secretase modulators target the transmembrane domain 1 of presenilin 1.** *Embo J* 2011, **30**:4815–4824.
11. Takagi S, Tominaga A, Sato C, Tomita T, Iwatsubo T: **Participation of transmembrane domain 1 of presenilin 1 in the catalytic pore structure of the gamma-secretase.** *J Neurosci* 2010, **30**:15943–15950.
12. Kukar TL, Ladd TB, Bann MA, Fraering PC, Narlawar R, Maharvi GM, Healy B, Chapman R, Welzel AT, Price RW, *et al*: **Substrate-targeting gamma-secretase modulators.** *Nature* 2008, **453**:925–929.
13. Kukar T, Murphy MP, Eriksen JL, Sagi SA, Weggen S, Smith TE, Ladd T, Khan MA, Kache R, Beard J, *et al*: **Diverse compounds mimic Alzheimer disease-causing mutations by augmenting Abeta42 production.** *Nat Med* 2005, **11**:545–550.
14. Beel AJ, Barrett P, Schnier PD, Hitchcock SA, Bagal D, Sanders CR, Jordan JB: **Nonspecificity of binding of gamma-secretase modulators to the amyloid precursor protein.** *Biochemistry* 2009, **48**:11837–11839.
15. Barrett PJ, Sanders CR, Kaufman SA, Michelsen K, Jordan JB: **NSAID-based gamma-secretase modulators do not bind to the amyloid-beta polypeptide.** *Biochemistry* 2011, **50**:10328–10342.
16. Herreman A, Serneels L, Annaert W, Collen D, Schoonjans L, De Strooper B: **Total inactivation of gamma-secretase activity in presenilin-deficient embryonic stem cells.** *Nat Cell Biol* 2000, **2**:461–462.
17. Watanabe N, Image I II, Takagi S, Tominaga A, Image Image I, Tomita T, Iwatsubo T: **Functional analysis of the transmembrane domains of presenilin 1: participation of transmembrane domains 2 and 6 in the formation of initial substrate-binding site of gamma-secretase.** *J Biol Chem* 2010, **285**:19738–19746.
18. Weihofen A, Binns K, Lemberg MK, Ashman K, Martoglio B: **Identification of signal peptide peptidase, a presenilin-type aspartic protease.** *Science* 2002, **296**:2215–2218.
19. Friedmann E, Lemberg MK, Weihofen A, Dev KK, Dengler U, Rovelli G, Martoglio B: **Consensus analysis of signal peptide peptidase and homologous human aspartic proteases reveals opposite topology of catalytic domains compared with presenilins.** *J Biol Chem* 2004, **279**:50790–50798.
20. Moehlmann T, Winkler E, Xia X, Edbauer D, Murrell J, Capell A, Kaether C, Zheng H, Ghetti B, Haass C, Steiner H: **Presenilin-1 mutations of leucine 166 equally affect the generation of the Notch and APP intracellular domains independent of their effect on Abeta 42 production.** *Proc Natl Acad Sci U S A* 2002, **99**:8025–8030.

21. Annaert WG, Esselens C, Baert V, Boeve C, Snellings G, Cupers P, Craessaerts K, De Strooper B: **Interaction with telencephalin and the amyloid precursor protein predicts a ring structure for presenilins.** *Neuron* 2001, **32**:579–589.
22. Brunkan AL, Martinez M, Wang J, Walker ES, Beher D, Shearman MS, Goate AM: **Two domains within the first putative transmembrane domain of presenilin 1 differentially influence presenilinase and gamma-secretase activity.** *J Neurochem* 2005, **94**:1315–1328.
23. Zhao G, Cui MZ, Mao G, Dong Y, Tan J, Sun L, Xu X: **gamma-Cleavage is dependent on zeta-cleavage during the proteolytic processing of amyloid precursor protein within its transmembrane domain.** *J Biol Chem* 2005, **280**:37689–37697.
24. Yagishita S, Morishima-Kawashima M, Tanimura Y, Ishiura S, Ihara Y: **DAPT-induced intracellular accumulations of longer amyloid beta-proteins: further implications for the mechanism of intramembrane cleavage by gamma-secretase.** *Biochemistry* 2006, **45**:3952–3960.
25. Hashimoto T, Wakabayashi T, Watanabe A, Kowa H, Hosoda R, Nakamura A, Kanazawa I, Arai T, Takio K, Mann DM, Iwatsubo T: **CLAC: a novel Alzheimer amyloid plaque component derived from a transmembrane precursor, CLAC-P/collagen type XXV.** *Embo J* 2002, **21**:1524–1534.
26. Qi-Takahara Y, Morishima-Kawashima M, Tanimura Y, Dolios G, Hirotani N, Horikoshi Y, Kametani F, Maeda M, Saido TC, Wang R, Ihara Y: **Longer forms of amyloid beta protein: implications for the mechanism of intramembrane cleavage by gamma-secretase.** *J Neurosci* 2005, **25**:436–445.
27. Okochi M, Tagami S, Yanagida K, Takami M, Kodama TS, Mori K, Nakayama T, Ihara Y, Takeda M: **gamma-secretase modulators and presenilin 1 mutants act differently on presenilin/gamma-secretase function to cleave abeta42 and abeta43.** *Cell Rep* 2013, **3**:42–51.
28. Urban S: **Taking the plunge: integrating structural, enzymatic and computational insights into a unified model for membrane-immersed rhomboid proteolysis.** *Biochem J* 2010, **425**:501–512.
29. Hu J, Xue Y, Lee S, Ha Y: **The crystal structure of GXGD membrane protease FlaK.** *Nature* 2011, **475**:528–531.
30. Li X, Dang S, Yan C, Gong X, Wang J, Shi Y: **Structure of a presenilin family intramembrane aspartate protease.** *Nature* 2013, **493**:56–61.
31. Monera OD, Sereda TJ, Zhou NE, Kay CM, Hodges RS: **Relationship of sidechain hydrophobicity and alpha-helical propensity on the stability of the single-stranded amphipathic alpha-helix.** *J Pept Sci* 1995, **1**:319–329.
32. Imamura Y, Watanabe N, Umezawa N, Iwatsubo T, Kato N, Tomita T, Higuchi T: **Inhibition of gamma-secretase activity by helical beta-peptide foldamers.** *J Am Chem Soc* 2009, **131**:7353–7359.
33. Das C, Berezovska O, Diehl TS, Genet C, Buldyrev I, Tsai JY, Hyman BT, Wolfe MS: **Designed helical peptides inhibit an intramembrane protease.** *J Am Chem Soc* 2003, **125**:11794–11795.
34. Takagi-Niidome S, Osawa S, Tomita T, Iwatsubo T: **Inhibition of gamma-secretase activity by a monoclonal antibody against the extracellular hydrophilic loop of presenilin 1.** *Biochemistry* 2013, **52**:61–69.
35. Asami-Odaka A, Ishibashi Y, Kikuchi T, Kitada C, Suzuki N: **Long amyloid beta-protein secreted from wild-type human neuroblastoma IMR-32 cells.** *Biochemistry* 1995, **34**:10272–10278.
36. Kan T, Tominari Y, Rikimaru K, Morohashi Y, Natsugari H, Tomita T, Iwatsubo T, Fukuyama T: **Parallel synthesis of DAPT derivatives and their gamma-secretase-inhibitory activity.** *Bioorg Med Chem Lett* 2004, **14**:1983–1985.
37. Li YM, Xu M, Lai MT, Huang Q, Castro JL, DiMuzio-Mower J, Harrison T, Lellis C, Nadin A, Neduvelil JG, *et al*: **Photoactivated gamma-secretase inhibitors directed to the active site covalently label presenilin 1.** *Nature* 2000, **405**:689–694.
38. Isoo N, Sato C, Miyashita H, Shinohara M, Takasugi N, Morohashi Y, Tsuji S, Tomita T, Iwatsubo T: **Abeta42 overproduction associated with structural changes in the catalytic pore of gamma-secretase: common effects of Pen-2 N-terminal elongation and fenofibrate.** *J Biol Chem* 2007, **282**:12388–12396.
39. Tomita T, Takikawa R, Koyama A, Morohashi Y, Takasugi N, Saido TC, Maruyama K, Iwatsubo T: **C terminus of presenilin is required for overproduction of amyloidogenic Abeta42 through stabilization and endoproteolysis of presenilin.** *J Neurosci* 1999, **19**:10627–10634.
40. Sato C, Takagi S, Tomita T, Iwatsubo T: **The C-terminal PAL motif and transmembrane domain 9 of presenilin 1 are involved in the formation of the catalytic pore of the gamma-secretase.** *J Neurosci* 2008, **28**:6264–6271.
41. Thinakaran G, Regard JB, Bouton CM, Harris CL, Price DL, Borchelt DR, Sisodia SS: **Stable association of presenilin derivatives and absence of presenilin interactions with APP.** *Neurobiol Dis* 1998, **4**:438–453.
42. Nyborg AC, Kornilova AY, Jansen K, Ladd TB, Wolfe MS, Golde TE: **Signal peptide peptidase forms a homodimer that is labeled by an active site-directed gamma-secretase inhibitor.** *J Biol Chem* 2004, **279**:15153–15160.
43. Kitamura T, Koshino Y, Shibata F, Oki T, Nakajima H, Nosaka T, Kumagai H: **Retrovirus-mediated gene transfer and expression cloning: powerful tools in functional genomics.** *Exp Hematol* 2003, **31**:1007–1014.
44. Tomita T, Maruyama K, Saido TC, Kume H, Shinozaki K, Tokuhiro S, Capell A, Walter J, Grunberg J, Haass C, *et al*: **The presenilin 2 mutation (N141I) linked to familial alzheimer disease (Volga German families) increases the secretion of amyloid beta protein ending at the 42nd (or 43rd) residue.** *Proc Natl Acad Sci U S A* 1997, **94**:2025–2030.
45. Watanabe N, Tomita T, Sato C, Kitamura T, Morohashi Y, Iwatsubo T: **Pen-2 is incorporated into the gamma-secretase complex through binding to transmembrane domain 4 of presenilin 1.** *J Biol Chem* 2005, **280**:41967–41975.
46. Morohashi Y, Kan T, Tominari Y, Fuwa H, Okamura Y, Watanabe N, Sato C, Natsugari H, Fukuyama T, Iwatsubo T, Tomita T: **C-terminal fragment of presenilin is the molecular target of a dipeptidic gamma-secretase-specific inhibitor DAPT (N-[N-(3,5-difluorophenacetyl)-L-alanyl]-S-phenylglycine t-butyl ester).** *J Biol Chem* 2006, **281**:14670–14676.
47. Hofmann K, Kiso Y: **An approach to the targeted attachment of peptides and proteins to solid supports.** *Proc Natl Acad Sci U S A* 1976, **73**:3516–3518.

doi:10.1186/1750-1326-9-7
Cite this article as: Ohki *et al.*: Binding of longer Aβ to transmembrane domain 1 of presenilin 1 impacts on Aβ42 generation. *Molecular Neurodegeneration* 2014 **9**:7.

OPEN ACCESS Freely available online

PLOS ONE

FTY720/Fingolimod, a Sphingosine Analogue, Reduces Amyloid-β Production in Neurons

Nobumasa Takasugi[1,2,3¤], Tomoki Sasaki[1], Ihori Ebinuma[1], Satoko Osawa[1], Hayato Isshiki[2,3], Koji Takeo[1], Taisuke Tomita[1,3]*, Takeshi Iwatsubo[1,2,3]

1 Department of Neuropathology and Neuroscience, Graduate School of Pharmaceutical Sciences, The University of Tokyo, Tokyo, Japan, **2** Department of Neuropathology, Graduate School of Medicine, The University of Tokyo, Tokyo, Japan, **3** Core Research for Evolutional Science and Technology, Japan Science and Technology Agency, The University of Tokyo, Tokyo, Japan

Abstract

Sphingosine-1-phosphate (S1P) is a pluripotent lipophilic mediator working as a ligand for G-protein coupled S1P receptors (S1PR), which is currently highlighted as a therapeutic target for autoimmune diseases including relapsing forms of multiple sclerosis. Sphingosine related compounds, FTY720 and KRP203 known as S1PR modulators, are phosphorylated by sphingosine kinase 2 (SphK2) to yield the active metabolites FTY720-P and KRP203-P, which work as functional antagonists for S1PRs. Here we report that FTY720 and KRP203 decreased production of Amyloid-β peptide (Aβ), a pathogenic proteins causative for Alzheimer disease (AD), in cultured neuronal cells. Pharmacological analyses suggested that the mechanism of FTY720-mediated Aβ decrease in cells was independent of known downstream signaling pathways of S1PRs. Unexpectedly, 6-days treatment of APP transgenic mice with FTY720 resulted in a decrease in Aβ40, but an increase in Aβ42 levels in brains. These results suggest that S1PR modulators are novel type of regulators for Aβ metabolisms that are active *in vitro* and *in vivo*.

Citation: Takasugi N, Sasaki T, Ebinuma I, Osawa S, Isshiki H, et al. (2013) FTY720/Fingolimod, a Sphingosine Analogue, Reduces Amyloid-β Production in Neurons. PLoS ONE 8(5): e64050. doi:10.1371/journal.pone.0064050

Editor: Koichi M Iijima, Thomas Jefferson University, United States of America

Received January 24, 2013; **Accepted** April 9, 2013; **Published** May 7, 2013

Funding: This work is supported in part by Grants-in-Aid for Young Scientists (S) (for T.T.) and (B) (for N.T.) from Japan Society for the Promotion of Science (JSPS), by the Grant-in-Aid for Scientific Research on Innovative Areas (Brain Environment) from the Ministry of Education, Culture, Sports, Science & Technology in Japan (for T.T.), by the Ministry of Health, Labor and Welfare of Japan (Comprehensive Research on Aging and Health) (for T.T.), by Core Research for Evolutional Science and Technology of JST (for T.T., T.I.). The funders had no role in study design, data collection and analysis, decision to publish, or preparation of the manuscript.

Competing Interests: The authors have declared that no competing interests exist.

* E-mail: taisuke@mol.f.u-tokyo.ac.jp

¤ Current address: Department of Pharmacology, Juntendo University School of Medicine, Tokyo, Japan

Introduction

Bioactive lipids, such as sphingolipids, have effect on various neuronal activities, including signal transduction, inflammatory response, and neuronal survivals [1]. It has been reported that the sphingolipid metabolism in brain was altered under neurodegenerative conditions, e.g., Alzheimer disease (AD) [2,3,4]. However, the relationship between changes in brain sphingolipids with the pathological mechanisms of AD has remained largely unclear. Interestingly, the production of amyloid-β (Aβ) peptide, the major component of senile plaques deposited in the brains of patients with AD, is known to be modulated by sphingolipids [5]. Aβ is produced from amyloid-β precursor protein (APP) through a sequential cleavage by two aspartate proteases, β- and γ-secretases [6,7]. BACE1 (β-site APP cleaving enzyme 1) [8] is a type-1 transmembrane protein responsible for the β-secretase activity, and γ-secretase is comprised of four integral membrane proteins, Presenilin (PS) as the catalytic subunit associated with Nicastrin (Nct), Aph1, and Pen2 [9]. Both enzymes are located in lipid rafts [10], a membrane microdomain enriched in sphingolipids and cholesterol, and the activities of the secretases are affected by the lipid composition [11,12,13].

Sphingosine-1-phosphate (S1P) is produced from sphingosine by sphingosine kinase (SphK). S1P works as a ligand for a subset of G-protein coupled receptor (S1PR) proteins, and functions on various cellular events including neurogenesis, angiogenesis, and immune response [14]. S1PR modulator FTY720 (Fingolimod/Gilenya) is a sphingosine-related molecule exhibiting an immunomodulatory function, which has recently been approved as an oral treatment for relapsing forms of multiple sclerosis [14,15]. FTY720 is phosphorylated by SphK2 to function as an agonist for S1P receptors, i.e., S1PR1, S1PR3, S1PR4, and S1PR5 (Fig. 1) [16,17,18]. Despite its agonistic action, FTY720 promotes endocytosis and degradation of the S1P receptors, thereby resulting in functional antagonistic effects. FTY720 interferes with the neuroinflammatory responses of auto-active T-cells and glial cells [19] and ameliorates the symptoms of autoimmune encephalomyelitis in rodents, the latter being a model for multiple sclerosis [20,21].

Recently, we reported that SphK2, one of the rate limiting enzymes for the production of S1P, is upregulated in AD brains, and that S1P interacts with BACE1 to regulate its proteolytic activity [22]. To examine the effects of S1P receptor modulators on AD, we investigated the effects of FTY720, and another S1PR modulator KRP203 harboring a more specific agonist activity against S1PR1 [23], on Aβ production in cultured neuronal cells and brain Aβ levels in AD model mice.

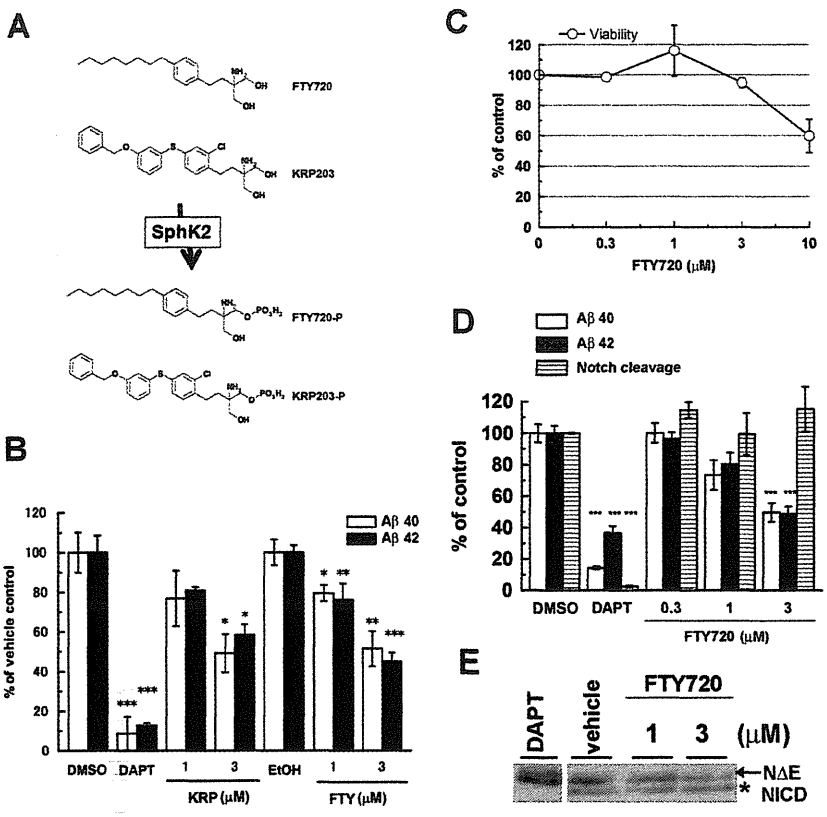

Figure 1. S1P receptor modulators, FTY720 and KRP203 decreased Aβ production from neuronal cells. (**A**) The chemical structures of FTY720 and KRP203 and their phosphorylated forms. (**B**) Levels of Aβ secretion from mouse primary neurons after treatment with FTY720 or KRP203 for 24 hrs. The levels of secreted Aβ in conditioned media were quantified by ELISAs. For vehicle control, we used DMSO for FTY720 treatment and EtOH for KRP203 treatment, respectively. The percentages of the relative ratio to levels in vehicle control of each group (mean ± SEM) are indicated in the figures. *P<0.05, ***P<0.001 by Student's t test. (n = 4). (**C**) Effects of FTY720 on cell viability in N2aNH cells. (**D**) Levels of Aβ secretion and Notch activity in N2aNH cells after treatment with FTY720 (n = 4, mean ± SEM; *P<0.05, **P<0.01, ***P<0.001). 10 μM of DAPT was used as a positive control. (**E**) Immunoblot analysis of NICD in FTY720-treated N2a cells, which was transiently transfected with cDNA encoding NΔE.
doi:10.1371/journal.pone.0064050.g001

Materials and Methods

Compounds

2-amino-2-[2-(4-octylphenyl)ethyl]-1,3-propanediol, hydrochloride (FTY720), 2-amino-2-[2-[2-chloro-4-[[3-(phenylmethoxy)phenyl]thio]phenyl]ethyl]-1,3-propanediol, hydrochloride (KRP203), 3-(2-(3-hexylphenylamino)-2-oxoethylamino) propanoic acid (W123), 5-[4-phenyl-5-(trifluoromethyl)-2-thienyl]-3-[3-(trifluoromethyl)phenyl]-1,2,4-oxadiazole (SEW2871) (Cayman chemicals), phosphorylated form of FTY720 (FTY720-P) (Echelon bioscience), and suramin (Sigma-Aldrich) were purchased from indicated venders. *N*-[*N*-(3,5-difluorophenacetyl)-L-alanyl]-(*S*)-phenylglycine *t*-butyl ester (DAPT) was synthesized as previously described [24]. FTY720, W123, suramin and DAPT were dissolved in DMSO. KRP203 and FTY720-P was dissolved in ethanol and chloroform, respectively.

Antibodies and immunological methods

A polyclonal antibody against presnilin1 (PS1) CTF (G1L3) was raised as described [25]. Following antibodies were purchased from indicated venders: 82E1 (Immuno-Biological Laboratories) against the N terminus of human Aβ for detection of Aβ and βCTF, anti-APP (C) (Immuno-Biological Laboratories) for detection of APP CTFs and AICD, anti-mouse/rat APP (597) for detection of sAPPα, anti-sAPPβwt (Immuno-Biological Laboratories), anti-α-Tubulin DM1A (Sigma Aldrich), anti-SphK2 P-19 (Santa Cruz Biotechnology), anti-Myc 9B11 and anti-phospho specific ERK antibody (Cell Signaling Technology). Protein samples were analyzed by immunoblotting or two-site ELISAs for the detection of Aβ as previously described [26,27]. Specificities of the APP antibodies used have previously been shown [22]. To analyze Aβ species with different C-terminal lengths, samples were separated by modified Tris/Tricine/8M urea gels as reported previously, followed by immunoblotting with 82E1 [28,29].

Cell culture and transfection

Expression plasmids coding for human APP C-terminal 99 amino acid fragment (pcDNA3.1-SC100), Notch C-terminal fragment (pCS2-NΔE), human Sphingosine kinase 2 (pcDNA3.1-SphK2-V5) and an inactive mutant of SphK2 (G243D) were described previously [22,26,30,31]. Plasmid transfection was performed using Lipofectamine2000 (Invitrogen). Stable mouse Neuro2a neuroblastoma cells line expressing recombinant Notch protein and luciferase reporter (N2aNH) was established by co-transfection with pcDNA3.1/Hygro-NΔE/gvp, pcDNA3-EGFP and pGL3(r2.2)-UAS [32,33] followed by selection with G418 and

hygromycin. After indicated time of treatment, medium and lysate were collected. To monitor the cell viability, we compared GFP fluorescence in each lysate with that of vehicle control samples. We further validated this viability assay using almarBlue assay (Invitrogen) (Figure S1). To monitor the Notch cleavage, luciferase assay was performed as described previously [29,32,33]. Primary cortical neurons were prepared from Balb/c mice at embryonic day 16, and grown in Neurobasal medium supplemented with B27 (Invitrogen) for 7 days [34,35]. Small interfering RNA (siRNA) duplexes targeting the mouse *Sphk2* sequence (target sequences: *Sphk2*: 5′-TAG GCC TGG CCT CGT TGC ATA-3′) as well as a negative control sequence were purchased from Qiagen. siRNA was reversely transfected in N2a cells using Lipofectamine RNAiMax (Invitrogen) as previously described [22]. cDNAs encoding NΔE [30] and NΔEgv [36] were originally provided from Drs. Raphael Kopan and Jan Naslund, respectively.

FTY720 treatment in AD model mice

All experiments using animals in this study were performed according to the guidelines provided by the Institutional Animal Care Committee of Graduate School of Pharmaceutical Sciences, The University of Tokyo. All animals were maintained on food and water with a 12 h light/dark cycle. A7 transgenic mice overexpressing human APP695 harboring K670N, M671L, and T714I FAD mutations in neurons under the control of Thy1.2 promoter were used as a mouse model of AD [37]. Female A7 mice at 6 months old were used for treatment of FTY720, in which FTY720 dissolved in saline was injected subcutaneously once a day for 6 days (0.5 mg/kg/day). Brain samples were solubilized with 10 mM Tris buffer containing 1% CHAPS, and subjected to the sandwich ELISA for Aβ (Wako Chemical) [22].

Results

S1P receptor modulators, FTY720 and KRP203, decreased Aβ production in neuronal cells

To test if the S1PR modulators alter Aβ production in neuronal cells, we treated mouse primary cortical neurons with FTY720 and KRP203 (structures shown in Figure 1A) and found that FTY720 and KRP203 decreased secretion of both Aβ40 and Aβ42 in a dose dependent manner (Fig. 1B). To further investigate the effect of these compounds, we tested a mouse neuronal N2a cell line stably expressing GFP, truncated Notch fused with Gal4/VP16 (NΔE/gvp) and a luciferase reporter under UAS promoter [32,33,36] (N2aNH cell line), which enables us to simultaneously analyze the effects of compounds on Aβ production, Notch signaling (as luciferase activity) and cell viability (as GFP fluorescence). Treatment with FTY720 decreased the production of Aβ40 and Aβ42 in a dose dependent fashion below the toxic concentration (Fig. 1C and S1) without affecting the Notch signaling (Fig. 1D and E).

To further identify the molecular target of S1PR modulators, we analyzed their effect on N2a cells transiently expressing SC100, corresponding to βCTF of human APP that is a direct substrate of γ-secretase. SC100 is endoproteolyzed by γ-secretase at ε-site to release the intracellular domain (AICD), and resultant intramembrane stub is trimmed by carboxypeptidase-like activity of the γ-secretase at multiple γ-sites to generate Aβ. FTY720 and KRP203 decreased secretion of Aβ40 and Aβ42 from SC100 (Fig. 2A), suggesting that S1PR modulators affected the γ-secretase activity. Recently, small compounds that specifically lower Aβ42, and Aβ40 to a lesser extent, have been termed as γ-secretase modulators [6,29]. However, FTY720 treatment decreased all Aβ species with different Aβ C-termini, including Aβ38, Aβ39, Aβ40 and Aβ42 (Fig. 2B). Concomitantly, a slight accumulation of αCTF (from endogenous mouse APP) and SC100 was observed (Fig. 2C–F), whereas the levels of sAPPα and sAPPβ products of α- or β-secretase-mediated APP cleavage of endogenous APP, respectively, were not altered by FTY720 treatment (Fig. 2G). Intriguingly, AICD production was not altered by FTY720 treatment (Fig. 2F) similarly to the processing of NΔE, a direct Notch substrate for γ-secretase (see Fig. 1D and E). Because both AICD and NICD are produced from ε-cleavage by γ-secretase, these data suggest that S1PR modulators specifically regulate the γ-cleavage irrespective of the substrate.

Mode of action of inhibition of Aβ production mediated by FTY720

Phosphorylation of FTY720 by SphK2 yields the active metabolite, FTY720-phosphate (FTY720-P), which is known as a potent agonist of the S1P receptors (Fig. 1A). To determine whether FTY720-P is involved in the regulation of Aβ production, we treated N2a cells with FTY720 after RNAi knock-down of the endogenous expression of SphK2. We observed a ~60% of decrease in SphK2 expression after siRNA treatment (Fig 3A). As reported previously, knockdown of SphK2 decreased Aβ secretion [22]. However, additional decrease was not observed in FTY720-treated SphK2 knockdown cells, suggesting that SphK2 is required for lowering Aβ secretion by FTY720 (Fig. 3B). Next, we examined the effects of overexpression of SphK2 or its dominant negative mutant (G243D) in N2a cells. As reported previously, overexpression of SphK2 increased Aβ production [22] (Fig. 3C). Intriguingly, FTY720 treatment significantly decreased Aβ secretion from N2a cells that overexpress wild-type (WT) SphK2, but not dominant negative mutant, to levels lower than those of untransfected cells treated by FTY720. Quantitative comparison of the inhibitory effects of FTY720 revealed that an increase in SphK2 activity significantly sensitized N2a cells to the inhibitory effect of FTY720 on Aβ production (Fig. 3D). These data strongly suggest SphK2 activity is involved in the mechanism of action of FTY720 to lower Aβ production, raising the possibility that FTY720-P is the *bona fide* regulator of the γ-secretase activities.

Phosphorylation of FTY720 by SphK takes place in the cytosol, and the resultant FTY720-P translocates to the extracellular side and acts as an agonist for S1PRs [38]. Next we examined whether known downstream signaling pathway of S1PRs was involved in the modulation of Aβ production. S1PR1, a major target of FTY720-P, is a Gi coupled receptor [39]. FTY720-P caused a significant phosphorylation of ERK1/2, a known downstream event of S1PR1-Gi signaling cascade (Fig. S2) in a similar fashion to that by SEW2871 [40]. Phosphorylation of ERK1/2 induced by SEW2871 was decreased by an authentic S1PR1 antagonist, W123 [41]. However, neither SEW2871 nor W123 affected the Aβ productions at indicated doses (Fig. S3). Then we tested co-treatment of W123 or suramin, the latter being known to work as a Gi protein inhibitor [42] together with FTY720. We found that both compounds failed to affect the decremental effect of FTY720 on Aβ production (Fig. 4A and B). In sharp contrast, extracellular addition of FTY720-P did not affect the Aβ production from N2a cells (Fig. 4C). These results raise the possibility that the molecular mechanism whereby FTY720 lowers Aβ production is independent of its antagonistic effects neither on S1PR1 nor Gi pathways and that intracellular FTY720-P lowers Aβ by an as yet identified mechanism.